Development of flexible biosensors for diagnostic applications

Isaac Aarón Morales Frias

Université Claude Bernard Lyon 1

THESE de DOCTORAT DE
L'UNIVERSITE CLAUDE BERNARD LYON 1

Ecole Doctorale N° 206
Ecole Doctorale de Chimie

Discipline : Chimie

Soutenue publiquement le 22/09/2023, par :
Isaac Aarón MORALES FRIAS

Development of flexible biosensors for diagnostic applications

---

Devant le jury composé de :

LEONARD, Didier, Professeur, Université Lyon 1	Président
BAUSELLS, Joan, Professeur, IMB-CNM,(CSIC, Espagne)	Rapporteur
KORRI-YOUSSOUFI, Hafsa, Directrice de Recherche CNRS Paris-Saclay	Rapporteuse
OLFA, Kanoun, Professeure, Université de technologie de Chemnitz (Allemagne)	Examinatrice
ERRACHID, Abdelhamid, Professeur, Université Lyon 1	Directeur de thèse
ZINE, Nadia, Maître de Conférences, Université Lyon 1	Co-directrice de thèse

This research was developed at the Micro & Nanobiotechnology Laboratory, Institut des Sciences Analytiques (UMR 5280) and Ecole Doctorale de Chimie (206) of the University Claude Bernard Lyon 1. Part of this work was performed in partnership with Integrated Graphene Ltd Eurohouse, Scottland, UK.

This dissertation contains results that were published (or submitted) in international scientific journals.

ACKNOWLEDGEMENTS

I would like to express my sincerest gratitude to my Ph.D. supervisor Prof. Abdelhamid Errachid and co-supervisor MCF. Nadia Zine for their invaluable support throughout the entire research and funding through the POC4allergies project.

Thank you to the staff at ISA (permanent and non-permanent), specially, Prof. Nicole Jaffrezic-Renault, Prof. Abdelhamid Elaissari, Dr. Francesca G. Bellagambi and Mme. Marie Hangouet for their support and constant motivation.

I want to thank my mom, dad, and sister for their encouragement.

Most significantly, thank you Marcos Portela for your strength, love, and support.

Thank you, God. Without you, none of this would have been possible.

PUBLICATIONS

Articles in international scientific journals

1. **Frias, I.A.M.**, Zine, N., Sigaud, M., Lozano-Sanchez, P., Caffio, M., & Errachid, A. (2023). Non-covalent π–π functionalized Gii-sense® graphene foam for interleukin 10 impedimetric detection. *Biosensors and Bioelectronics*, 222, 114954. **IF:12.5**
2. **Frias, I.A.M.**, Zine, N., Sigaud, M., Lozano-Sanchez, P., Caffio, M., & Errachid, A. (2023). Impedimetric NT-proBNP Aptasensor Based on SPCE and Maleimide Click Chemistry. Submitted to *Biosensors and Bioelectronics*.
3. **Frias, I.A.M.,** Ruankham, W., Zine, N., & Errachid, A. (2023). Impedimetric Microsensor for Cardiac Insufficiency Based in Single-Step Binding of LASIC Modified Anti-NT-proBNP Antibodies. Submitted to *Biosensors and Bioelectronics*.
4. **Frias, I.A.M.,** Zine, N., Moghbel, M., Brandt, K.J., & Errachid, A. (2023). Impedimetric Antiphospholipid Syndrome Diagnosis Based on Electrodeposited Click Chemistry. Submitted to *Biosensors and Bioelectronics*.
5. Ruankham, W., **Frías, I.A.M.**, Phopin, K., Tantimongcolwat, T., Bausells, J., Zine, N., & Errachid, A. (2023). One-step impedimetric NT-proBNP aptasensor targeting cardiac insufficiency in artificial saliva. *Talanta*, 124280. **IF: 6.5**
6. Hilali, N., Ruankham, W., **Frías, I.A.M.**, Bellagambi, F., Hangouet, M., Martin, M., ... & Errachid, A. (2023). Copper-free click chemistry assisted antibodies for immunodetection of interleukin-10 in saliva. *Microchemical Journal*, 1(1), 1. **IF: 5.3**
7. Montoro-Leal, P., **Frías, I.A.M.**, Vereda, E., Errachid, A., & Jaffrezic-Renault, N. (2022). A molecularly imprinted polypyrrole/GO@ Fe3O4 nanocomposite modified impedimetric sensor for the routine monitoring of lysozyme. *Biosensors*, 12(9), 727. **IF: 5.7**
8. Razmshoar, P., Bahrami, S. H., Rabiee, M., **Frias, I.A.M.**, Hangouet, M., Martin, M., ... & Jaffrezic-Renault, N. (2022). An impedimetric immunosensor based on PAMAM decorated electrospun polystyrene fibers for detection of interleukin-10 cytokine. *Journal of Electroanalytical Chemistry*, 926, 116953. **IF: 4.5**
9. Merzouk, S., **Frias, I.A.M.,** Bausells, J., Sigaud, M., Jaffrezic-Renault,N., Errachid, A. & Zine, N. (2023). All solid-state poly(vinyl chloride) membrane ion-selective microelectrodes with single wall carbon nanotube solid internal contact. Submitted to *Electroanalysis*.

Oral communications in international conferences

1. **Frías, I.A.M.**, Montoro-Leal, P., Vereda, E., Errachid, A., & Jaffrezic-Renault, N. Lysozyme molecularly imprinted impedimetric biosensor based on electrodeposited polypyrrole/GO@Fe3O4. *Réunion d'automne du Club Microcapteurs chimiques*, France 24th-25th November 2022.
2. **Frías, I.AM.,** Zine, N., Sigaud, M., Lozano-Sánchez, P., Caffio, M., Errachid, A. Microfluidic lab-on-chip device for simple impedimetric monitoring of il-10. *Summer school on smart devices and their applications*, Germany, 4th-8th June 2023.

ABSTRACT

Electrochemical biosensors are competitive diagnostic devices from conception, ready to discern biochemical and physicochemical signals. Notwithstanding the enormous amount of transduction methods produced to evaluate and monitor clinical anomalies, their profitable implementation depends on their integration with miniaturized flexible systems in which, polymeric substrate, transducer surface modification, bioelectronics, and fluid control at the interior of microfluidic chambers are some of many variables that require close examination to be determined and to control the immobilization of bioactive probes, target detection and flushing away. In this thesis we explore the development of chemical modification methodologies to enhance the electronic properties of carbon-derived materials and electrodeposition of click chemistry molecules over gold sputtered surfaces to be used as transducers in alternative clinical diagnostics. We fabricated integrated microfluidic systems designed to provide automated incubation, measurement, and cleaning. The electrodes were prepared with graphene foam directly grown on polyimide substrates by a catalyst-free method without the use of a transfer process. Chemical functional groups were provided by chemisorption of pyrene derivatives with carboxyl moieties. Graphene electrical properties were maintained because its crystalline structure was not modified. As a result, the devices showed detection at the femtogram range. Although graphene foam-based electrodes show very good electrochemical response in comparison to regular screen-printed carbon electrodes (SPCE), their price is more elevated. For this reason, in another approach, we included outstanding biological strategies to enhance SPCE response. Briefly, pyrene maleimide was covalently tethered to the substrate through π-π interactions and the maleimide group was used for the specific click chemistry with thiolated oligonucleotide aptamers. Finally, we continued to explore the maleimide click chemistry reaction as a quick and efficient method to develop biorecognition layers in biosensors. The electrografting of diazonium salts over gold has been reported to be fragile or weak because the electrocatalytic reaction stops after the first cycle. Here we present optimized electrodeposition parameters allowing the monolayer deposition of amino phenyl maleimide. The highly oriented film allowed us to immobilize orientation-dependent protein epitopes while maintaining their biological function. In this thesis we show how integrated biosensors could bring forth advantages to medical services by easing the patient's experience in regard of sample collecting while working parallel to current clinical diagnostic methods without demanding specialized laboratories and monitoring the clinical evolution of a patient who can now be followed in real-time even for long-term follow-up.

RESUME

Les biocapteurs électrochimiques sont des dispositifs de diagnostic prêts à discerner les signaux biochimiques et physicochimiques. Malgré l'énorme quantité de méthodes de transduction produites pour évaluer et surveiller les anomalies cliniques, leur mise en œuvre dépend de leur intégration avec des systèmes flexibles miniaturisés dans lesquels le substrat polymérique, la modification de la surface du transducteur, la bioélectronique et le contrôle des fluides à l'intérieur des chambres microfluidiques sont de variables qui nécessitent un examen attentif pour être déterminées et pour contrôler l'immobilisation des sondes bioactives, la détection des cibles et leur évacuation. Dans cette thèse, nous explorons le développement de méthodologies de modification chimique conçues pour améliorer les propriétés électroniques des matériaux dérivés du carbone et l'électrodéposition de molécules de chimie clic sur des surfaces pulvérisées en or afin d'être utilisées comme transducteurs dans des diagnostics cliniques alternatifs. Nous avons fabriqué des systèmes microfluidiques intégrés conçus pour fournir une incubation, une mesure électrique et un nettoyage automatisé. Les électrodes ont été préparées avec de la mousse de graphène directement cultivée sur des substrats en polyimide. Les groupes fonctionnels chimiques ont été fournis par chemisorption de dérivés du pyrène avec des groupes carboxyle. Les propriétés électriques du graphène ont été conservées car sa structure cristalline n'a pas été modifiée. En conséquence, les appareils ont montré une détection dans l'ordre du femtogramme. Bien que les électrodes à base de mousse de graphène présentent une très bonne réponse électrochimique par rapport aux électrodes de carbone sérigraphiées classiques (SPCE), leur prix est plus élevé. Pour cette raison, dans une autre approche, nous avons inclus des stratégies biologiques exceptionnelles pour améliorer la réponse SPCE. En bref, le pyrène maleimide était lié de manière covalente au substrat par le biais d'interactions π-π et son groupe maléimide a été utilisé pour la chimie click spécifique avec des aptamères oligonucléotidiques thiolés. Enfin, bien que l'électrogreffage de sels de diazonium sur de l'or s'est avéré fragile ou faible car la réaction électrocatalytique s'arrête après le premier cycle, nous présentons ici des paramètres d'électrodéposition optimisés permettant le dépôt monocouche hautement orienté qui nous a permis d'immobiliser des épitopes protéiques dépendants de l'orientation tout en conservant leur fonction biologique. Dans cette thèse, nous montrons de solutions intégrées qui pourraient surveiller l'évolution clinique des patients en temps réel et long terme.

CONTENT

LIST OF ABBREVIATIONS

SCs- Semiconductors

PCB- Printed Circuit Boards

VOCS- volatile organic compounds

IL-10 – Interleukin 10

NT-proBNP- N terminal Pro-Brain Natriuretic Peptide

SPCE- Screen printed carbon electrodes

eV- Electron volts

EIS- Electrochemical impedance spectroscopy

CV-Cyclic voltammetry

In the last 20 years, a big percentage of biosensor research has been performed in solid state materials such as gold, metal oxides and layered semiconductors (SCs) wired within circuitries in PCB boards. However, one of the current and most practical scope of biosensor research is to develop easy-to-use monitoring applications as point-of-care devices. In these conditions, the electronic and physicochemical properties of these complex substrates seem too specialized and expensive for a single use biosensor from which thousands are expected to be used in a single day in primary health services.

Single use monitoring biosensors should be designed in cheap single-use substrates. Plastic, aluminum, paper, and other recyclable materials seem like a good choice for preparing biosensing substrates and devices. However, since total recycling is not possible and, if biosensors are ever expected to be used extensively, biodegradable substrates need to be developed or adapted so the final ecological impact of biosensors can be close to zero. Some of the popular materials being currently developed as transducers for biosensing applications are gold discs, carbon, silicon, and other metal oxide semiconducting materials. Because of their hard mechanical properties, these materials cannot be easily transferred to thin polymeric substrates that are intrinsically flexible. For that reason, we need to develop transducing materials that are adapted to bending and compression without cracking.

Under normal conditions of use, flexible biosensors are designed for working in an unobtrusive manner as self-integrated devices embedded within a flexible framework. With them, analyzing body fluids could be performed in an unintrusive manner. These body fluids hand out a great amount of metabolic information in the form of biomarkers such as ions (e.g., Na^+, K^+, Ca^+, and Cl^-), small molecules (e.g., cortisol, glucose, lactate, uric acid, peptides, and ammonia), and volatile organic compounds (VOCS). All these biomarkers are of special clinical interest and can be used to monitor metabolic diseases and disorders. For instance, monitoring interleukin 10 (IL-10) is essential for understanding the vast responses of T-cells in cancer, autoimmunity, and internal homeostasis after physical stress. On another example, we have NT-proBNP, a prohormone secreted by the heart when its tissue is affected by chronical swealing. The presence of high levels of antibodies toward specific proteins in the blood can also indicate metabolic unbalance, such as the increasing presence of anti-phospholipid antibodies are associated to lowest live birth rate and increased incidence of preeclampsia, intrauterine growth restriction and stillbirth.

The integration of microfluidics with monitoring biosensors may automate the measurement and treatment of biological samples. These devices can have a positive impact on health services and in the daily life of the patients because they collect the sample and incubation, washing and measuring flux can be regulated by programed pumps. With this strategy, flushing of biological samples can be directed to a sealed bag for easy sterilization. Furthermore, microfluidics is essential for miniaturized electrochemical biosensors because, at low volumes, the ionic or redox probe used to perform the measurement can be quickly exhausted during measurement, which rends the measurement unreliable.

In this thesis, carbon-based transducers deposited over flexible polymeric substrates were studied, and new methods of chemical functionalization were developed to enhance their electronic properties. Graphene is a carbon nanomaterial known for its outstanding conductivity, however, its use in biosensors frequently requires the creation of functional groups over its crystalline lattice (most commonly carboxyl groups). In this case we developed a non-covalent functionalization strategy by availing graphene's sp^2 electronic π cloud to couple other molecules sharing the same property. With this strategy, we can dope graphene with carboxyl functional groups without disrupting its precious conductive properties. As a result, the impedimetric measurements can be performed in saline buffer, an ecologic solution well known by health services and that does not require specialized waste treatment.

Although, pure semiconducting nanomaterials such as graphene excel in their function as conductive transducers that can be adapted over flexible substrates, its high price is still regarded as a drawback for its generalized use in monitoring biosensors. On the other hand, screen printed carbon electrodes (SPCE) are cheaper and already possess oxygen-containing functional groups to the detriment of the electronic qualities of the carbon ink. To overcome this disadvantage, we developed an electrochemical conditioning method for SPCE to reduce oxidated defects found over the active surface of the printed ink. With its reconditioned electronic properties, SPCEs were enabled for π-π functionalization strategy to implant maleimide click-chemistry functional groups. Although the electronic properties of the carbon ink were enhanced, they were not at the level of pure graphene transducer. For this reason, we incorporated specific oligonucleotide aptamers as an outstanding biological strategy to mediate fast electron transfer by migration of charge from the double-layer capacitance to the carbon transducer. It is with these two strategies that commercial SCPE were enhanced to detect at the femtogram range in complex serum samples.

Gold is another material that can be adapted to flexible substrates. Its sputtering over polymeric sheets can be performed rather easily with specialized equipment, and it is strong

when adapted chemical treatment is performed onto the surfaces. However, the chemical modification of gold is rather limited to the adsorption of free thiol groups or electrodeposition of diazonium salts, which is regarded as unstable because the success of the electrochemical reaction varies with the intrinsic electronegativity of the modified phenyl molecule. Despite of this, its utility cannot be disregarded for some of its properties are well aligned to the requirements of wearable biosensors. For instance, pristine carbon-based materials are challenged to oxidize most common analytes being that its work function goes around 4.3~ 4.7 eV depending on its thickness (one to ten monolayers), because of this, it presents slow electron transfer kinetic. On the other hand, the work function of gold is around 5 eV, which also largely matches the valence band edge of most p-type SC with faster electron kinetics. For these reasons, we include exploratory research for this material while maintaining the scope on click chemistry functional groups. We aimed to develop and optimize a method for the electrodeposition of maleimide diazonium salts over gold substrates. For this study, solid state silicon microchips featuring evaporated gold working electrodes were used as a standard device to find the optimized conditions to be implemented in gold evaporated flexible substrates. We optimized the physicochemical and electrical parameters needed to fabricate layer-by-layer deposition of maleimide groups over the surface.

The research presented in this thesis represents technological groundwork that can be easily transferred to other flexible substrates. This work provides different options to enhance the electrochemical response of carbon-based materials (pure or inks) as well as a reproducible methodology to provide gold thin films with homogeneous layer-by-layer maleimide click chemistry groups specific for thiol binding, which provides spatial organization and complete surface passivation. In future works, the challenge will be more focused in four main challenges: the first one, developing biodegradable polymers for wearable or implantable applications for *in situ* monitoring of the concentration of different biomarkers. Secondly: the integration of flexible biochemical sensors with implantable soft electronics. Thirdly: combining electrochemical energy storage devices or self- power supply for autonomous wearable and implantable biochemical sensors. The final development is expected to assist the current healthcare system profile to be preventive, predictive, participatory, and personalized.

ORGANIZATION OF THE THESIS

The objective of this thesis is to explore the development of flexible biosensors integrated in a microfluidic device, and the chemical modification of carbon and metal transducers while maintaining their electronic properties. We studied the stability and biological function of immobilized biomolecules, antibodies, and oligonucleotide aptamers. In Chapter 1 we present general bibliography about biosensors as alternative to current analytic clinical diagnostics, the development of flexible biosensors including, the transducer, the substrate, the kind of bodily fluids that can be analyzed, examples of flexible immunosensors and the challenges associated to their integration in microfluidic devices. In Chapter 2, we present published results about a flexible graphene-based immunosensor and the fabrication of a 3-D printed microfluidic device featuring a clasping structure with resin-printed internal tubing which directs the fluids into the electrode chamber. In Chapter 3, we present how we overcome the challenge of using flexible screen-printed carbon electrodes by enabling them for click chemistry to thiol groups. The biosensor was integrated in a miniaturized microfluidic lab-on-chip device designed for impedimetric monitoring in a portable potentiostat that can be connected to a cellphone. In Chapter 4 we present a procedure to electrograft maleimide diazonium salts over sputtered gold substrates to continue the exploration of click chemistry reactions as a quick and efficient method to develop robust biorecognition layers. In Chapter 5 we conclude with general discussion, conclusion and perspectives emerging from this work.

CHAPTER 1

GENERAL BIBLIOGRAPHY

1. Biosensors as alternative to current analytic clinical diagnostics

Clinical analyses are performed in laboratory centrals at the primary health care level. If the healthcare unit is of private service, the access to these analyses must be covered by the patient at an elevated cost and, if a public service is involved, a health professional should confirm its necessity and, depending on the health service's budget, the access can be finally granted or not. Current stablished laboratory tests are expensive for they are performed in sophisticated instruments or employ complex methodologies and highly trained personnel to perform them. Because of this, decision makers have set rules and conditions a patient should fulfill to be granted with the right of the analysis. As a result, chronic diseases are diagnosed at an advanced stage or, because of the high demand, emergency care is delayed. Indubitably, primary health care requires cheaper and faster methods to diagnose and perform patient sorting to make the most efficient use of the limited resources they are assigned to.

More recently, COVID-19 pandemic changed the paradigm of clinical diagnosis. We have been acquainted to a new kind of fast clinical diagnosis which are acquired on the pharmacy and performed by ourselves. These lateral flow diagnostics are also knowns as biosensors. However, biosensors have been around us during the last 70 years in the form of electrochemical glucometers for diabetic persons, for example. We can notice that biosensors are alternatives to laboratory analysis, they are being developed with the objective of being pre-prepared diagnostics, ready and easy to use. As a more complex example of biosensors, we can think of the enzyme-linked immunosorbent assay (ELISA kit), which has become a current stablished gold standard test.

The development of any biosensor requires multidisciplinary knowledge, starting by the identification of a molecule of relevant clinical interest (biomarker), and a deep study of its physicochemical stability and biological function. A biosensor comprises four main components, as follows: (1) the target biomarker, whose chemical or structural characteristics will be used for its detection and quantification; (2) the biorecognition element, a biomolecule receptor with high affinity towards the target analyte (e.g., enzymes, antibodies, oligonucleotides, aptamers, cells, proteins, etc); (3) the transducer, which aims to convert the bio(recepetor/marker) interaction into a measurable signal, proportional to the concentration of the biomarker present in the clinical sample; and, (4) a signal-processing system for the transducer signal (normally an electronic equipment design to translate the signal produced by the transducer and PC) (Naresh and Lee, 2021).

Biosensors can be classified in terms of their biorecognition element (immunosensors, aptasensors, whole-cell-sensors, etc.). Based on their transducing method, they can be classified

as electrochemical, optical, and mass-based biosensors, among others (Purohit et al., 2020). Mass-based biosensors (gravimetric) employ techniques such as crystal quartz balance for piezoelectric biosensors and magnetostrictive microcantilever for magnetoelectric biosensors. Optic-based biosensors require the use of spectrometers or surface-plasmon resonance, for example. Finally, electrochemical biosensors employ electrical techniques such as amperometry, conductimetry, potentiometry, and impedance spectroscopy. Optical and electrochemical detection methods are preferred for biosensing devices used in clinical applications. For instance, optical biosensors depend on the use of a label for signal amplification which can be chromatic or fluorescent molecules, nanoparticles of oxide materials to be used as contrast agents in imaging methods or metallic nanoparticles in the case of plasmon-based and Raman-based signal-processers. However, the sensitivity of optical transduction methods depends on the technological development of optical devices with improved photon counting while the electrochemical ones depend on the transducing layer which determines the effectiveness of the electrochemical method. Current electrical technology can measure very small currents in the order of 10^{-12} Amperes (pA), around 6.25 million electrons per second. For these reasons, the electrochemical approach is most appealing for biosensing and bioelectronics research (Frías et al., 2015).

Over the last 20 years, solid substrates such as gold and glassy carbon discs have been the standard substrates used to characterize the biological interaction between biomolecules in solid-state immobilization. Because of the conductive or semiconconductive properties of these substrates and the requirement that biomolecules have for an aqueous environment; the development of electrochemical biosensors is the indisputable answer to the dilemma. Electrochemical methods are preferred for the construction and development of biosensors due to their sensitivity, rapid analysis, and direct interpretation. In addition, technological advancements in material sciences and electronics have paved the way for the development of miniaturized electrochemical biosensors.

Biosensing applications must be developed to perform fast and accurate measurements of biomarker levels as they are indicators of the functioning of biological processes, pathogenic processes, or the result of therapeutic interventions. At the same time, the result should be easily readable and interpreted by a technician or by the patients themselves, and most importantly, these devices should be low-cost. The classification of the electrochemical biosensors is presented in Table 1. All these biosensors have miniaturization potential and can be associated with cloud computing and the internet of things (IoT), favoring the sharing of results for decision-making guided by medical doctors and skilled personnel (Pateraki et al., 2020).

Table 1. Classification of the electrochemical biosensors (Ensafi, 2019).

Classification	Description
Potentiometric	Measures the potential difference caused by the concentration gradient resulting from the biosensor-analyte interaction, whose reaction occurs mainly at the interface of the working electrodes.
Amperometric	The reaction occurs by measuring the current as a function of the applied potential or time, resulting in oxidation/reduction of electroactive species in two or three-electrode configurations.
Conductometric	It quantifies the conductivity variation in two-electrode systems resulting from the electrochemical reaction produced by the detection of analytes.
Impedimetric	It measures the electrical impedance of a system at the biosensor-electrolyte interface. In this case, a low-amplitude AC voltage is applied to measure the current as a function of frequency on the functionalized electrode.

Among the electrical characterizations that can be performed with this type of biosensors, we have potentiometric and amperometric measurements. In potentiometric measurements, an electrochemically active solution is used to help quantify the difference in potential between two electrodes, a working electrode, and a reference electrode. The difference in potential is measured due to the oxidation and reduction of electroactive species in the solution. In amperometric measurements, a time-varying potential is applied, and as a result, electrochemical oxidation, or reduction of one of the electroactive species occurs. This kind of measurement is performed using 3 electrodes, in them, current flows between the working electrode and the auxiliary, and its response is measured against the reference electrode.

For most biosensors, interface characterization can be performed by impedance spectroscopy, studying the change in polarization when an applied voltage is reversed. Applying a single-frequency voltage or current to the interface allows measuring the phase shift and amplitude of the resulting current at that frequency using an equivalent circuit to analyze the response (Macdonald and Barsoukov, 2018). Impedance is the time-varying resistance measured at the interface after short electrical stimuli are applied as a step function of voltage over time. The resultant perturbations must be mathematically analyzed through Laplace or Fourier transformation to associate them with the frequency domain. In practical instrumentation, single-frequency voltage or current (within 1mHz and 1MHz) is applied to the

interface and the phase shift and amplitude are transformed as real and imaginary parts of the impedimetric response of the resulting current at each frequency. The chosen frequency range is determined by the nature of the solid-liquid interfaces of the biosensor and their time constants. For instance, in Fig.1 we can see that slow aqueous diffusion processes which generally have relatively large time constants (on the order of 0.1–10s) can be analyzed at frequencies between a few millihertz and 100kHz. On the other hand, studies of the ionic motion at the solid transducing layer (milli- to microseconds), require higher frequencies between a few hertz and 3-15 MHz to measure their time constants.

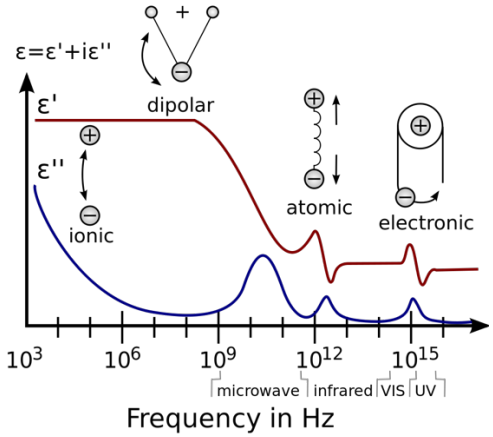

Figure 1. Dielectric permittivity spectrum over a wide range of frequencies. (From the dielectric spectroscopy page of the research group of Dr. Kenneth A. Mauritz. http://www.psrc.usm.edu/mauritz/dilect.html)

Impedimetric biosensors are studied by electrochemical impedance spectroscopy technique (EIS) in a similar way to amperometric measurements, however, semiconducting materials or transducers with lower electrical conductivity are used. The advantage of using this type of material is related to the decrease in electronic permeability, which is smaller and allows a more detailed analysis of the quantitative parameters and their electrocapacitive properties. To analyze the electrical response of these sensors by the EIS technique, we can use a Nyquist plot (Fig.2), in which the impedance spectrum represents the dependence of the imaginary and real components of the impedance (Z" vs Z') as the applied frequency varies. Soon after, the electrical responses (in the form of semicircles) are associated with an electrical circuit. The chosen circuit is the one whose mathematical model fits the result of the Nyquist plot, which is then called an equivalent circuit. Electrochemical reactions known for the transfer of electrons at the electrode surface, involve electrolyte resistance, adsorption of electroactive species, and charge and/or mass transfer on the electrode surface. Each reaction process can be represented by the elements of the electrical circuit consisting of resistors, or constant-phase elements (CPE)

combined in parallel or series. The most studied model of the electrical circuit for a simple electrochemical reaction is the Randles-Ershler electrical equivalent circuit model, which includes the resistance of the electrolyte solution (R_s), the charge transfer resistance of the electrolyte at the electrode/electrolyte (R_{CT}), the capacitance that occurs at the electrical double layer interface (C_{dl}), and the mass transfer resistance which when developing freely is also known as Warburg diffusion. Finally, each parameter of the equivalent circuit corresponds to the processes occurring at different regions of the actual biosensor according to their distance from the surface of the electrode. Regularly, magnitude changes in parameter R_{CT}, or the CPE are sufficiently large between samples to allow their differentiation in relationship with the amount of captured mass.

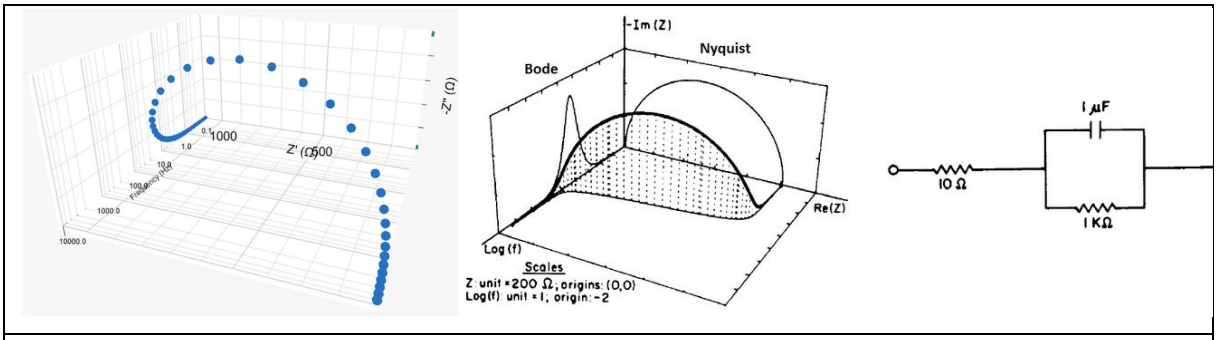

Figure 2. 3D projection plot of the impedance spectroscopy response in terms of frequency and face shift (Bode plot) and equivalent circuit. (AN-EIS-001Metrohm 2019 and (Macdonald et al., 1981))

2. Development of flexible biosensors.

2.1.Historical evolution of the field

The first reported biosensor was an enzyme-based electrode for glucose detection reported by Clark and Lyons in 1962 (Clark Jr. and Lyons, 1962). In Fig. 3, we present some examples of the technology developments of their device over the last 70 years. Their prototype device can be seen as a first generation of biosensing probes based on glucose oxidase entrapped within a semipermeable dialysis membrane which was constructed inside a glass oxygen electrode. Second generation biosensors are technological enhancements of the first commercial biosensor, and interdisciplinary research in electrochemical biosensors aims to improve their characteristics and performance, in addition to miniaturize the overall systems to make them suitable for cheap, mass production. Advancements in surface chemistry, screen-printing technologies and semiconductor integration technologies combined with the use of synthetic electron acceptors resulted in major advances in the development of home-use

commercial electrochemical glucose biosensors (Ross et al., 1990). Screen printing technologies are now being adapted to produce disposable, small or miniaturized, robust and cheap electrodes for electrochemical biosensors.

Figure 3. 70 years of development of electrochemical glucometers.

Nowadays, flexible, stretchable, and wearable biosensors for point-of-care (POC) testing are rapidly creating a billionaire research market. In addition, there is a considerable number of published reviews discussing new aspects of the flexible sensing market in wearable devices, functional textiles, electronic skins, and flexible bio and optoelectronics (Ates et al., 2022; Wang et al., 2023). Going forward to the third generation of biosensors, the focus is on the wiring of biological probes to the transducer, therefore, minimization of the electron-transfer distance is crucial to increase the performance of the sensor. In this sense, nanoscience and nanotechnology has taken over the field of biosensors and bioelectronics to avail some of the highly desirable features of nanomaterials and apply them as transducers. For instance, carbon-based nanomaterials such as carbon nanotubes and graphene have given rise to major advances in the field. Because of their electrical, chemical, and mechanical properties, carbon nanomaterials are becoming an essential component of many biodetection technologies. The size and dimensions of nanostructures such as gold nanoparticles and carbon nanotubes are compatible with biomolecules, consequently such nanomaterials are being used to establish a bridge between the electrode and the biorecognition events as electrical connectors that might enable or improve electron transfer.

2.2. Polymeric substrates and their properties

If biosensors are expected to be used by everyone, and in large quantities, it is important to think about waste disposal and treatment. For these reasons, characteristics like light weight, flexibility and recyclability are important for the industrial production of electrochemical biosensors, so their transport and disposal can be facilitated with small impact on the ecology.

The selection of the substrate depends on the requirements of a particular application, i.e., where the biosensor is intended to be used. Ultrathin plastic substrates like poly(ethylene terephthalate) (PET), poly(ethylene naphthalate) (PEN), and polyimide (PI), possess intrinsic polymeric properties (mechanical and temperature stability). Moreover, materials such as polycarbonate (PC), polyurethane (PU) and PET are highly deformable and optically transparent. Of note, biosensors prepared in flexible substrates are intended to be used inside cuvettes, chambers, or microfluidic devices and therefore, characteristics arising from the substrate's polymeric properties such as elasticity, thickness and light weight are more valuable than the flexible property itself. Nonetheless, once polymeric substrates have shown good results, other technological approaches can be implemented to put in use their flexible property. For instance, in the case of skin wearable applications, substrates require shape memory and low elastic modulus at large mechanical deformations. These kinds of flexible devices are conceived for interface non-invasive sampling/analysis of body fluids like sweat, saliva, and tears. Recent research is focused on developing biocompatible platforms with similar mechanical properties like human skin (Liu et al., 2023). In addition, the materials used as transducers must avoid biocompatibility issues resulting from the attachment of the flexible sensor onto the epidermis. To construct a flexible sensing device, an ultrathin flexible substrate with properties of stretchability, roughness, surface energy, thickness, thermal stability, mechanical stability, and stability to fit with the nonplanar structure of the human body is highly desirable (Lin et al., 2022).

Engineering polymeric substrates is essential to increase the scope of electrochemical biosensors, nanomaterials can be included in the substrate to enhance their mechanical properties. For instance, stretchable and flexible membranes produced with polydimethylsiloxane (PDMS) have had their mechanical strength features enhanced by the addition of Carbon nanotubes (CNTs) (Zhang et al., 2018). On another example, polyvinylalcohol/alginate membranes have been implemented with conductive polyaniline to produce blood plasma filtration membranes that can be analyzed in real time by EIS (Frias et al., 2021). Another aspect to consider is that controlling hydrophilicity and hydrophobicity in substrates is also important for the fabrication of the biosensor. For instance, high surface energy indicates high hydrophilicity, therefore strong adhesion properties between the substrate and transducer. Lower surface energy relates to low hydrophobicity, an important characteristic that enhances the resolution of printing patterns by effect of reduced lateral spread of inks (Sreenilayam et al., 2021).

2.3.The transducer's material

Recent scope of the research field in conductive materials scours for soft, flexible, and light properties that are in conformity with the mechanical characteristics of polymeric substrates. These kinds of electrochemical transducers are needed for flexible electronics, and they can be grouped by cost-effectiveness, robustness, fast response time, and low work volume. The field has been developing quickly because current knowledge about transducing materials is being adapted to biocompatible and biodegradable flexible substrates to promote the development of lightweight, portable, bendable, implantable biomedical devices, and wearable biosensors (Bocchetta et al., 2020).

Because of their large area to volume ratio, nanomaterials have shown to improve the analytical features of electrochemical biosensors. For instance, carbon nanomaterials (carbon nanotubes, graphene, and carbon black) and metallic nanomaterials (noble metal and metal oxides) have demonstrated electrocatalytic activity and biocompatibility (Narayanan et al., 2020; Wu et al., 2021). Graphene stands out from other carbon nanomaterials because its conductivity is higher than carbon nanotubes, and it can be used as an active channel, dielectric, or conductive electrode. Its planar sp^2 hybridization promotes π-π electronic conjugation over long distances, therefore it presents high electrical conductivity. Top quality graphene is produced at small amounts from micromechanical cleavage, anodic bonding, photo exfoliation, liquid phase exfoliation, growth from silicon carbide, precipitation from metal, chemical vapor deposition, molecular beam epitaxy and chemical synthesis from benzene rings (Vasilijević et al., 2023). It has been shown that both graphene monolayer and polylayer films are uniform in work function from 4.30 to 4.70 eV (Rut'kov et al., 2020). The main challenge of using pure graphene is its low water dispersibility thus, the choice of the appropriate solvents or surfactants are crucial since graphene is highly hydrophobic. The most common strategy is to introduce polar oxygen groups to its basal plane in detriment of its electronic properties. Oxidation of the graphitic crystal produces defects mainly in the borders of the nanostructures; in this way, the electronic conduction is preserved but with a low number of anchoring sites. Further intense oxidation results in the creation of more functional groups, although the holes in the conductive crystal decrease the overall electronic conductivity. To improve the limited electronic properties of graphene oxide (GO), other conductive and capacity active materials can be blended (metal oxides, metal sulfides and silicon) (Dai et al., 2020), however the cost increase and loss of mechanical properties are a drawback for their application in flexible biosensors.

Other materials like gold can be engineered with film-producing techniques like chemical coating, chemical or physical vapor deposition, and sputtering. Although these

materials can be adapted for flexible applications, they are not easily employable in stretchable films. For optical applications, clear transducers might be interesting, however, gold, and other metallic films are not transparent even in the form of nanometer thick films (Costa et al., 2019). Nanotechnology can help produce flexible, stretchable, and transparent metals in different geometries, such as nanowires, nanoparticles, and metallic liquid conductors. Gold nanoparticles have also been used to modify carbon screen-printed electrodes (SPCEs); however, the results are not very promising because they are reported to cause higher background noise (Nelis et al., 2020). Nevertheless, gold electrodes are often employed as the source, drain, and gate electrodes because the work function of gold is around 5.0 eV, which matches the valence band of p-type semiconductors (Watanabe et al., 2022).

Semiconducting polymers exhibit π-electron delocalized backbones with band gaps that can be tuned by carefully selecting the monomers used for polymerization. For this reason, this kind of non-conventional polymers can accomplish electronic transducer applications effectively. Their physicochemical properties can be enhanced through nanotechnology or by their synergistic combination with nanomaterials to develop original properties such as high conductivity, high electron transfer kinetics, charge storage capacity, structural flexibility, environmental stability, low cost, and simple fabrication protocols. However, few of them present functional groups (-COOH or -NH_2) to bind bioreceptors. Thus, drawbacks such as low solubility and long-term instability can be fixed, giving rise to innovative composites useful in bioelectronic devices (Heeger, 2010).

Over the last 10 years, the micro and nano biotechnology (MNBT) group has developed specialized chemistry for many different transducers, and currently, some of them are internally considered as development models (Fig. 4). Evaporated gold transducer is often used over the last layer of silicon-based 4-plotted microchips. The microchip features a 4 × 7mm silicon transducer integrated with four gold working electrodes (WE= 0.64 mm2), two Ag/AgCl reference electrodes (RE = 0.13 mm2), and a central platinum counter electrode (CE= 1.37 mm2). Silicon technology fabricated in a clean room at the Institute of Microelectronics of Barcelona (IMB-CNM) uses a 10 cm diameter silicon wafer. The first layer is composed of an 800 nm thick silicon dioxide layer grown by thermal oxidation. Subsequently, the metallic areas confined for electrodes are fabricated by physical vapor deposition, photolithography, and lift-off, as follows: Gold-WE features a triple layer with 50 nm Ti, 50 nm Ni, and 200 nm Au layers. Platinum-CE is fabricated in a bilayer with 15 nm Ti and 150 nm Pt. Silver-RE is fabricated in a bilayer with 15 nm Ti and 150 nm Ag. The microchip is treated with plasma-enhanced chemical vapor deposition to fabricate a dielectric bilayer consisting of 400 nm SiO_2 and 400

nm of Si_3N_4. Photolithography and dry reactive ion etching are used to remove the passivation layer from the active microelectrodes area. Finally, the microchip is wire-bonded to a PCB using Kulicke and Sofa 4523A equipment and insulated using Ep-Tek H70E-2LC epoxy resin (Hilali et al., 2023).

In another development performed at the IMB-CNM, hafnium oxide (HfO_2) was used to increase the thermal stability of silicon. Atomic layer deposition (ALD) uses deionized H_2O as the oxygen precursor, together with tetrakis(dimethylamido)-hafnium for HfO_2 deposition and N_2 as the carrier/purging gas. Deposition of the HfO_2 layer is carried out at a temperature of 225 °C and at a base pressure of 300 mTorr using 100 ALD cycles (Lee et al., 2012).

More recently, a partnership with Integrated Graphene Ltd., provided graphene microelectrodes. Graphene foam was directly grown on polyimide substrates by a catalyst-free method without the use of a transfer process. Graphene was *insitu* embedded onto polyimide films by laser treatment. In this electrode, the counter and working electrode are graphene foam, and the reference electrode is solid contact Ag/AgCl. The working electrode diameter area is 4 mm with a 1 mm space between the counter electrode which surrounds it in a C format. To complete the system, the Ag/AgCl reference electrode is placed below the working electrode, and as a continuation of the counter electrode, maintaining 1 mm of separation.

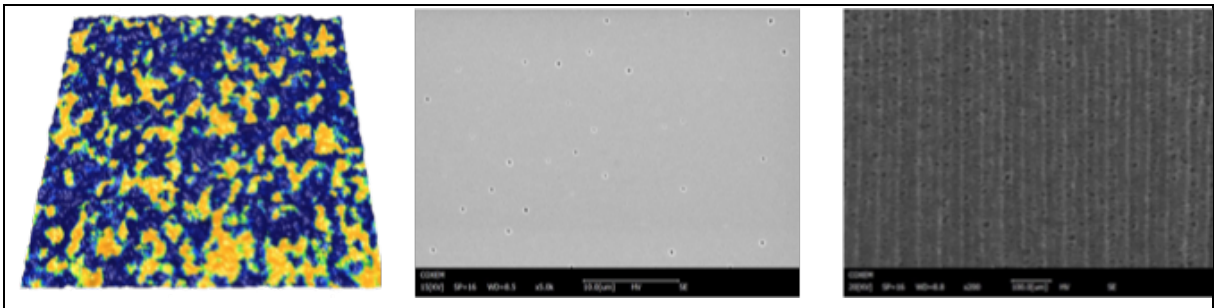

Figure 4. Different transducers for electrochemical biosensors, from left to right, hafnium oxide, gold and graphene foam.

As we can notice, fabricating final product flexible biosensors requires several development stages. The study of superficial phenomena occurring at the interface of the substrate/transducer and that to the biorecognition layer must be characterized in model electrodes with already proven electrochemical performance. In the MNBT group plasma evaporated metal semiconductor microchips manufactured over printed circuit (PCB) boards are being used to characterize surface chemistry functionalization and the biorecognition events (Fig. 5). Once the measurement parameters have been optimized, the bio/chemical strategies can be transferred to prototype microelectrodes to be studied. In Figure 4 we show some of the substrates used to hold the transducing layer. Most of the substrate materials use for

electrochemical transducer have similarities such as semiconducting abilities of silicon and polyimide.

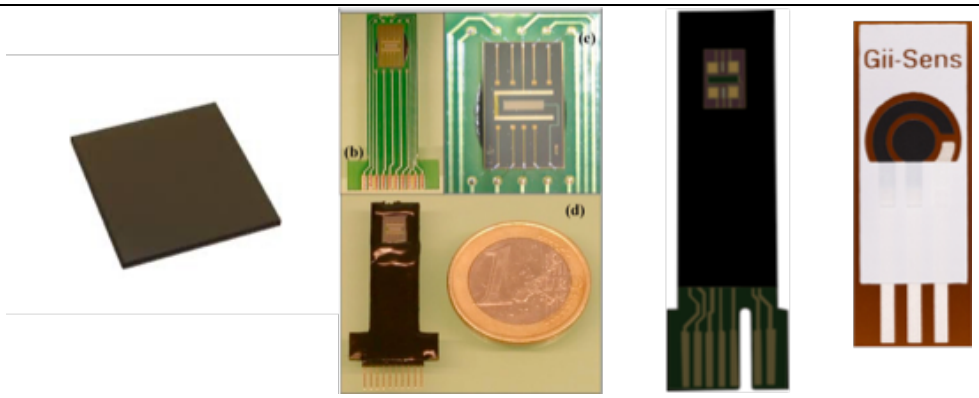

Figure 5. Substrate for transducing materials, hafnium oxide, evaporated gold over electrode microchips and graphene foam.

2.4. Transducer functionalization for anchoring the recognition molecule

Electrochemical biosensors for clinical diagnosis applications are mostly constructed over solid conducting or semiconducting surfaces. Most transducing surfaces lack functional binding groups to tether specific biological probes. Of note, because of the metallic electron cloud, π-cloud, electronic conjugation or the presence of weak physicochemical interactions, transducing surfaces can bind nonspecifically to a great number of biological molecules due to strong driving forces in biological complexation processes. However, biosensors require to be highly sensitive to detect low abundance of analytes and selective enough to perform the detection in the presence of interaction interferents. Mainly, there are two main modification strategies to improve the quality of surfaces, i.e., to increase their sensitivity to a single biological interaction. Antifouling coatings are used to reduce background noise by hindering unspecific binding to the surface, on the other hand, amplifying coatings are designed to favor the biointeraction of the analyte with the surface by increasing the amount of bound specific biological probe.

Blood plasma contains over 80 g/L of proteins (Frutiger et al., 2021) and within it, albumin acts as chaperon molecule creating stable complexes by hydrophobic binding. This same effect can be translated to antifouling coatings to provide the blocking of hydrophobic nonspecific binding sites over the biosensing surface, and to suppress the toxicity of nanomaterials when testing *in vivo* systems. In addition to albumin, surface fouling is mostly prevented by blocking hydrophobic surfaces by the addition of strongly hydrated polar

molecules such as ethylenediamine and zwitterionic polymers such as poly(ethylene glycol) (PEG) and oligo(ethylene glycol) (OEG).

Biosensors translate a biomolecular recognition or binding event into an electric measurable signal. To enhance or amplify the response signal, many strategies can be followed. For instance, glucose enzymatic biosensors are based on an enzymatic reaction which generates a measurable electric current. Most other electrochemical biosensors depend only on the specific binding interaction between the analyte and a receptor; thus, the response signal comes from a reduction-oxidation (redox) probe such as ferrocyanide/ferricyanide ($[Fe(CN)_6]^{4-}$/ $[Fe(CN)_6]^{3-}$), whose redox reaction will occur at the surface of the transducer. Depending on the amount of material bound to the surface and its intrinsic charge, the diffusion rate of the redox probe might be hindered or increased. Most commonly, a blocking effect will take place and thus, after a biointeraction, an increased amount of mass over the surface will increase impedance and even decrease the overall conductivity of the transducer. To get better accurate results, it is preferred to attach covalently the biological probe layer to prevent leaching and degradation throughout the fabrication steps (incubations and washing steps). Many strategies for immobilizing bioreceptors adopt strong-interaction immobilizations (covalent, through amide, maleimide coupling reactions) and non-covalent interactions (electrostatic attraction, π-π stacking, entrapment and conjugation). Other immobilization strategies such as crosslinking, physicochemical conjugation, and chemical immobilization have also shown very good results which demonstrates the resilience of biomolecules to functional and activation treatments (Luo and Davis, 2013). For instance, glutaraldehyde reacts with the amine group of proteins playing the role of cross-linker due to the high activity of its two OH groups. The activation method using EDC/NHS occurs on carboxylic acids followed by an amidation reaction. The main advantage of the later is its high conversion efficiency and mild reaction conditions and biocompatibility (Zhang et al., 2008). In this sense, modifying transducing substrates through functionalization with EDC/NHS is an effective strategy to modulate its biofunctional properties to help anchor biomolecules. For instance, interdigitated gold microelectrodes with PEDOT-polyallylamine hydrochloride films have been used to fabricate electrochemical devices.

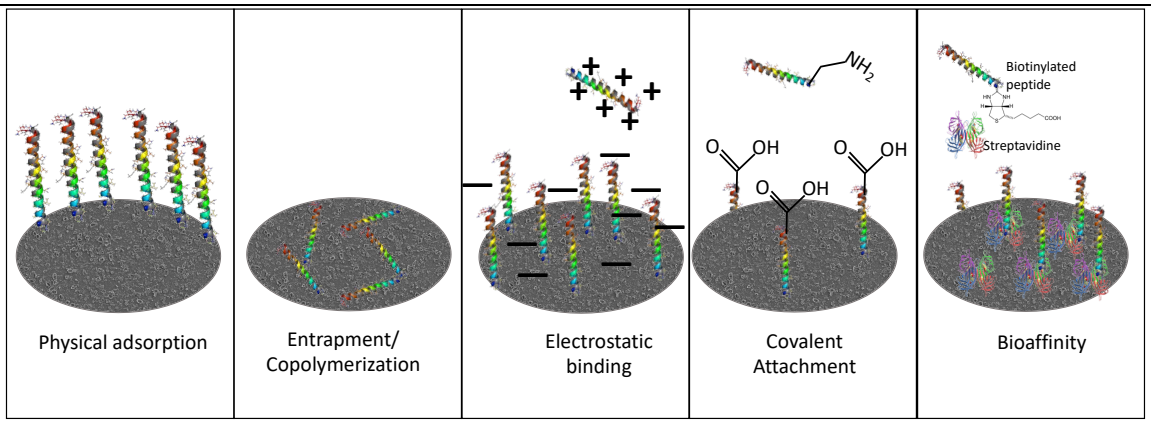

Figure 6. Main methods for anchoring the recognition biomolecule

In Fig. 6, we show the main methods used for anchoring the biomolecule probe. Physical adsorption is a fast procedure that does not involve chemical steps, however, lacks reproducibility and stability of the bioreceptor due to lack of biocompatibility. Entrapment or copolymerization relies in synthesized polymeric matrices associated with the bioreceptor to provide a favorable environment for the immobilization of high number or probes, obtaining chemical stability in a single process. Despite the lack in stability, electrostatic binding results in immobilization from the interaction of electrically charged polymeric surfaces. Covalent attachment is the immobilization resulting from an activated surface and functional groups of the bioreceptor, a relatively laborious procedure; however, it provides stability and reproducibility. Biological affinity has elevated recognition by pair of biomolecules such as streptavidin biotin binding. A wide range of bioreceptors and surfaces can be easily functionalized with these molecules.

2.5. Choice of the biorecognition molecule

In nature, biomolecular differentiation is performed by controlling the local concentration of biomolecules through compartmentalization and via the binding affinity of an interaction (Stein et al., 2009). Specificity relates to the preferential binding to one molecule over another, even in heterogeneous concentrations. This means that after the binding interaction between a pair of complementary biomolecules, the complexation leads to a metastable state of reduced energy. The term specific binder is relatively defined by stereospecificity and shape complementarity (Frutiger et al., 2021). However, if similar competitors are present during the recognition event, the overall binding affinity will determine the successful binding event. On the other hand, a nonspecific binder is a molecule presenting

a binding interface where two molecules can interact in multiple ways without stereospecificity and shape complementarity.

During the development of biosensors specific binding is desired. However, in most cases a probe can bind to multiple partners, these interactions can be functional or nonfunctional. For instance, cross-reaction is a nonfunctional kind of binding, it occurs when a probe binds to a target it was not designed for. Another thing to consider is the association rates of biomolecules, the binding will occur at this rate until a plateau (which will be considered the affinity constant) is reached. This kinetic behavior describes the association and dissociation of the complex during an interaction time.

Antibodies and aptamers are known as probes with specific molecular recognition. For its part, antibodies are blood proteins produced by some cells during the exposure to a nocuous antigen. The performance of antibodies varies from batch to batch, and when used, the environmental conditions of the binding should be reoptimized every time. They are sensitive to temperature and can easily undergo irreversible denaturation. However, when an unknown antigen gains popular research interest, the production of immunoassays is the first choice to start studying its detection and quantification. Furthermore, once the right antibody has been selected, current advances in monoclonal antibodies production can produce micro and nanobodies, i.e. paratopes attached to small nonimmunogenic proteins. On the other hand, compared in some of the concepts that we just stated, oligonucleotide aptamers can be considered superior to antibodies because of their quick production, uncomplicated chemical modification, and structural consistency between batches. Aptamers are smaller in size than antibodies and are generated by the systematic evolution of ligands by exponential enrichment (SELEX) to a broad spectrum of target molecules (antigens). Although aptamers are raised in the presence of a single antigen, the information regarding the affinity and selectivity properties of the aptamer-target complexes are not always available due to incomplete characterization of the selected aptamer (Jayasena, 1999), not to mention that their pharmacokinetic properties are largely unknown.

In another aspect of choosing the biorecognition molecule, one should consider the chemistry and physico-chemistry of the surface where the probe will be attached. For instance, if a hydrophobic surface is being used (such as graphene), oligonucleotides and more hydrophilic antibodies most be used, in this way, the different forces around the probe will help to point them perpendicular to the surface, amplifying the probabilities of catching its affinity analyte.

2.6. Sample: Body fluids

Blood is the most common sample taken in a clinical analysis. Blood plasma represents around 55%, while red cells and white blood cells represent 45%. Plasma is about 92% water, and the main plasma protein groups are albumins, globulins, and fibrinogens. The primary blood gasses are oxygen, carbon dioxide, and nitrogen. Plasma without fibrinogen is named serum. In this solution we also find amino acids, proteins, carbohydrates, lipids, hormones, vitamins, electrolytes, dissolved gasses, cellular wastes, abundant endogenous and foreign biomarkers, and pathogenic agents of many diseases. Therefore, the construction of highly effective biosensors to monitor specific biomarkers in blood or serum is vital for clinical diagnosis, and the development of flexible electrochemical biosensors is promising in achieving minimally invasive sampling and sensing (Bar et al., 2020).

Saliva is a blood ultrafiltrate rich in similar physiological components. However, it allows noninvasive sampling and is a straightforward procedure different from blood collection. In addition, most analytes in saliva present higher stability over time. As a drawback, there are many other interferents in saliva, including bacteria and food residuals. Therefore, it is necessary to pretreat the saliva samples by centrifugation to remove some disturbances from saliva before detection (Vozgirdaite et al., 2021).

Urine is another relatively easy to collect sample and contains a variety of components, such as uric acid, urea, creatinine, inorganic salts, organic acids. Urine biomarkers reflects the final metabolism and is useful for monitoring drug intake, in addition to cancer diagnosis (Smith et al., 2020).

Other important samples, although difficult to collect are, cerebrospinal fluid (CSF) which represents the physiological environment for the human brain and contains many physiological biomarkers such as neuropeptides, proteins, and neurotransmitters that are important for monitoring anxiety, depression, and neurological diseases such as Parkinson's disease (Fame and Lehtinen, 2020). Another one is interstitial fluid (ISF), the fluid circulating within the cells, it transports signaling biomolecules, nutrients and metabolites between cells, blood, and the lymph through capillary exchanging effect; microneedles are needed to obtain this fluid (Kim and Prausnitz, 2021). Other body fluids with a smaller number of biomarkers are tears and sweat. Nevertheless, using this samples is interesting because no puncturing or dicing is required to obtain them. Therefore, developing monitoring flexible biosensors for these fluids will offer gently sampling and in situ minimally invasive analysis of biological samples.

The composition of body fluids including blood serum, cerebrospinal fluid (CSF), and interstitial fluid (ISF) vary with the physiological state of our organism. According to the WHO, the term biomarker includes any measurement reflecting an interaction between a biological system and a potential hazard, which may be chemical, physical, or biological. The measured response may be functional and physiological, biochemical at the cellular level, or a molecular interaction (Strimbu and Tavel, 2010). In this sense, the levels of antibodies, proteins, enzymes, and other biomolecules that can reflect the actual state of human physiology are important elements for clinical diagnosis.

2.7.Biomarkers in relation with diagnostic of disease

According to the National institute of Environmental Health Sciences, a biomarker is an objective measure that captures what is happening in a cell or an organism at a given moment. There are many reviews addressing biomarkers that have different classifications for them (Laterza et al., 2007; Levenson and Melnikov, 2013) and many others can be found with specifical scope for a disease or organ. For the scope of this thesis, we can narrow down the concept of biomarkers as the subset of molecules that can be objectively measured, evaluated as indicators of homeostasis, pathogenic processes, or a pharmacological response to a therapeutic intervention.

During the last fifty years, the link between soluble factors and disease gave way to the discovery of many biomarkers. Heart failure biomarkers were slowly discovered by microscopic observations of atrial heart tissue and later purification and sequencing of atrial peptides of varying sizes that possessed natriuretic, diuretic, and/or smooth muscle relaxing activity (Potter et al., 2009). Similarly, the discovery of cytokines was performed from neutrophils from the peritoneal cavity of ill rabbits presenting fever. The biological properties of these soluble factors included fever, resistance to viral infections, elevated white blood cell count, the synthesis of acute phase proteins, death of cancer cells and migration of inflammatory cells (Dinarello, 2007). The interleukin nomenclature relates to their biological properties, and according to Dinarello, At the time of naming these molecules with an interleukin number, primary amino acid sequences of the active molecules were not known. For instance, IL-1 was used to define a monocyte product and the term IL-2 was used to define a lymphocyte product. In the early 90s, Th2 cells was discovered which inhibited cytokine synthesis, especially IFN-y production, by Thl cell clones. This activity was initially described as cytokine synthesis inhibitor factor and has now been designated IL-10 (de Waal Malefyt et al., 1992).

Nowadays biomarkers are discovered and studied by using genomics, proteomics, lipidomics and molecular profiling in drug development. Because of technical advancements in these platforms, it is possible to study the expression profile of thousands of genes, gene products, and small molecules (Tebani et al., 2020). It is expected that biomarkers will be useful in understanding the underlying pathophysiological processes of diseases and thus help drug development.

3. Polymeric flexible electrochemical biosensors.

The growing demand on specific biosensors is good news for primary health services, at the same time, is alarming due to the gigantic amount of solid, chemical, and electronic waste that their fabrication and use would generate (Chaudhary et al., 2023). To reverse the imminent impact of biosensors on the ecology, the packaging and biosensors architecture should be improved with eco-friendly components and materials. In this context, polymeric biosensors are being produced as prototypes to monitor physical and physiological parameters related to human health determined to attain sustainable global development goals. Once developed on polymeric substrates, electrochemical biosensors possess the distinct advantage of being easy to transport in large quantities, simple to discard and to recycle.

With the use of polymeric substrates, transducers must be adapted to their flexible characteristic. Because of their mechanical strength and flexibility, nanomaterials including graphene, carbon nanotubes (CNTs), metal nanowires and conductive polymers are being used as transducers for the construction of polymeric flexible sensors. Within these lines, new or adapted flexible transducers are challenged by the requirements of biological probes, for instance, the orientation of the biological probes after immobilization. For instance, EDC/NHS activation chemistry enables tethering of antibodies through the amine group found in the base of the variable portion of the antibody. Despite this method is good enough and allows covalent immobilization of the antibody, it does not ensure the accurate orientation of the immobilized antibody to detect its antigen. Glutaraldehyde (GA) reacts with the amine group of proteins playing the role of cross-linker due to the high activity of its two OH groups and, at the same time, it serves as a spacer from the transducer bestowing more degrees of freedom to the biological probe, however without preferential orientation. Other immobilization strategies such as crosslinking, physicochemical conjugating, and chemical immobilization have also shown good results demonstrating the resilience of biomolecules. The proximity of the biological prove to the transducer is also critical, for instance, the biorecognition can produce

changes in potential, current, capacitance, or impedance. A variety of analytes from the clinical field can be effectively detected by the coupling between immunological reactions and electrochemical methodologies. The net electric polarity charge of either antibodies or antigen is correlated with the ionic composition of the solution and the isoelectric points of components. Impedimetric biosensors rely on detecting impedance changes at the interface of the electrode before and after the biorecognition, these variations can be correlated to the concentration of the analyte present in sample solution (Mathew et al., 2021).

Most flexible electrochemical biosensors are developed over transducer-coated plastic sheets, nonetheless, recent research include the encapsulated multi-walled carbon nanotubes (MWCNTs) in polydimethylsiloxane (PDMS) films (Liu et al., 2021). On another example, deposited reduced graphene oxide over PET has exhibited good conductivity and a considerable number of oxidated groups available for the immobilization of biological receptors by the EDC/NHS activation chemistry (Gwiazda et al., 2022). Furthermore, flexible platinum electrodes have been fabricated onto Bio-PET surfaces by conventional photolithography, characterized, and applied for the detection of biomarkers related to Parkinson's disease (Oliveira et al., 2020) and flexible screen-printed immunosensor based on silver electrodes sprayed with SWCNTs layers (Shkodra et al., 2020). More recently, *in situ* growth of graphene over polymeric films, have paved the way for easy and manufacturing of flexible carbon sensors (Lin et al., 2014), however, zero bandgap graphene is known for being hydrophobic and thus, unsuitable for direct use as a transducer in biosensing devices. Therefore, some oxidation of its crystalline lattice is still required to make it a functional material (Ye et al., 2018).

In the MNBT group, flexible microelectrodes have been constructed over polyimide by a combination of soft lithographical tools including microcontact printing (μCP) and self-assembled monolayers (SAMs) (Fig. 7). The devices were sealed with PDMS to create a microfluidic system.

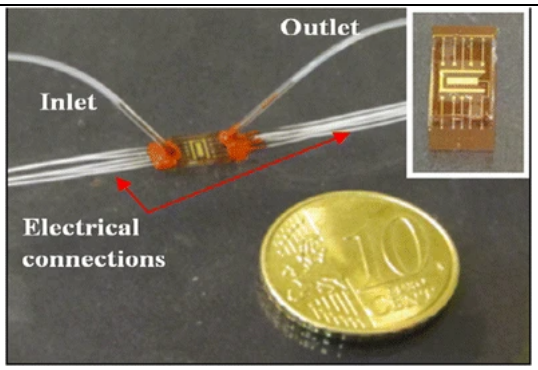

Figure 7. Image of the final μLoC on PI substrate connected to electrical wires for EIS measuements with an inlet and outlet from both sides of the μLoC for electrolyte circulation through the window of analysis

To conclude this topic, we found that the current strategy to develop flexible biosensors is impregnation of plastic sheets with conductive materials for their further chemical modification. However, these methodologies might not create robust transducing layer with the ability to resist several incubation and washing steps. On the other hand, selection of dynamic specific probes demands the design of soft chemistry processes that promote their immobilization while granting preservation of their bioactivity. The *insitu* growth of graphene is a promising technique for the fabrication of flexible carbon microelectrodes and, as we will show in this thesis, avoiding the disruption of the chemical stability of the graphene transducer grants the immobilization of bioreceptors by non-covalent strong physicochemical interactions such as electrostatic attraction and π-π stacking.

4. Microfluidic integration.

The accomplishment of flexible biosensors anticipates the practical identification of several specific targets of clinical interest in real-time, hence the need for multi-detection devices. In this sense, electrode miniaturization and microfluidics architecture play strategic parts in their design to ensure incubation, target detection and flushing away. Despite the number of transducers developed to tether functional biological probes, their profitable implementation depends on their integration with microelectromechanical systems. Electrode composition and size, fluid velocity profile and pressure distribution at the interior of the microfluidic chamber are some of many variables that require close examination to control the immobilization and stability of biomolecules. The integration of microfluidics can overcome the issues that compromise data integrity and, at the same time, upgrade sample collection and measurement by improving sample transport for better temporal resolution and accuracy (Gao et al., 2023). Microsystems are particularly challenging because they require direct contact between sample fluids and electrodes. One major challenge is the topographical conflict between electrical connections and microfluidic channels. Microfluidic methods include active flux such as dielectrophoresis, magnetic, and acoustic. Passive microfluidic methods are related to the flux using the characteristics of the samples such as density and surface tension (Liang et al., 2020). Moreover, channel confinement plays a dominant role in the squeezing regime and inhibits capillary instability (Zhu and Wang, 2017).

Stereolithography, is a relatively low-cost 3D printing technology used to construct any tool under specification. It employs a photocurable polymeric resin which hardens when exposed to a focused light beam. Printing materials such as resins possess varying optical properties, strength, and chemical resistance to provide the best strategy for fabrication. In the case of biomedical applications, medical-grade resins are being used to fabricate human prosthetics (dental and orthopedic). For these reasons, 3D printing is a promising technique for the fabrication of microfluidic diagnostic devices because they are designed to reduce handling and employing minimal volumes without altering the composition of the biological sample. Moreover, integrated microfluidics should use low binding or medical-grade materials to reduce contamination between samples from large molecules and cellular or tissue components.

Although some microfluidic systems are obtained by simple connecting tygon tubes to a polymeric plate, geometrically complex microfluidic prototypes with pre-treatment or mixing chambers can be easily designed with the aid of 3D design software (Yan et al., 2018). In Fig. 8 we show an example of an optimized microfluidic device. On the left, the original model designed by integrated graphene Ltda, used for electrochemical measurements and to the right, the optimized version for electrochemical impedance spectroscopy measurements. Performing trustable EIS measurements requires to perform a calibration curve by the standard addition method and therefore, performing several repetitions of the electrical measurement at each point until stabilization of the double-layer capacitance. At every measurement, the ionic probe used to obtain the electrochemical response degrades and eventually, exhausts. Therefore, the use of single drops of ionic solution to measure EIS spectra for biological samples is not recommended. In such a way, the optimization performed over the left model consists of the inclusion of a microfluidic chamber fed by a slow and continuous flux of ionic solution which grants the interchange of exhausted solution without altering the stability of the double layer capacitance.

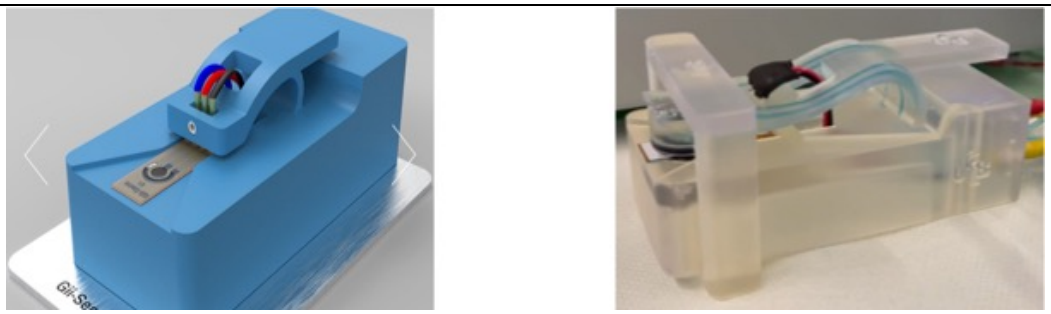

Figure 8. 3D modelling of improved integrated microfluidic system for sensor reading before and after.

The design of 3D printed microfluidic devices can be performed according to the needs of sample processing of the biosensors, providing cheap, miniaturized, multifunctional and sensitive diagnostic devices. With the help of the printed prototypes, biosensors can easily become final diagnostic tools to be used in health services or at home. 3D printing technology still needs improvement to include functional materials like conductive inks and biomimetic substrates. In addition, the use of different materials with diverse physical properties or even the inclusion of bioactive materials without compromising their basic activity, would improve the applicability of multisensing devices.

5. References.

Ates, H.C., Nguyen, P.Q., Gonzalez-Macia, L., Morales-Narváez, E., Güder, F., Collins, J.J., Dincer, C., 2022. End-to-end design of wearable sensors. Nat Rev Mater 7, 887–907. https://doi.org/10.1038/s41578-022-00460-x

Bar, N., Korem, T., Weissbrod, O., Zeevi, D., Rothschild, D., Leviatan, S., Kosower, N., Lotan-Pompan, M., Weinberger, A., Le Roy, C.I., 2020. A reference map of potential determinants for the human serum metabolome. Nature 588, 135–140.

Bocchetta, P., Frattini, D., Ghosh, S., Mohan, A.M., Kumar, Y., Kwon, Y., 2020. Soft Materials for Wearable/Flexible Electrochemical Energy Conversion, Storage, and Biosensor Devices. Materials. https://doi.org/10.3390/ma13122733

Chaudhary, V., Rustagi, S., Kaushik, A., 2023. Bio-derived smart nanostructures for efficient biosensors. Curr Opin Green Sustain Chem 42, 100817. https://doi.org/https://doi.org/10.1016/j.cogsc.2023.100817

Clark Jr., L.C., Lyons, C., 1962. ELECTRODE SYSTEMS FOR CONTINUOUS MONITORING IN CARDIOVASCULAR SURGERY. Ann N Y Acad Sci 102, 29–45. https://doi.org/https://doi.org/10.1111/j.1749-6632.1962.tb13623.x

Costa, J.C., Spina, F., Lugoda, P., Garcia-Garcia, L., Roggen, D., Münzenrieder, N., 2019. Flexible Sensors—From Materials to Applications. Technologies (Basel). https://doi.org/10.3390/technologies7020035

Dai, C., Sun, G., Hu, L., Xiao, Y., Zhang, Z., Qu, L., 2020. Recent progress in graphene-based electrodes for flexible batteries. InfoMat 2, 509–526. https://doi.org/https://doi.org/10.1002/inf2.12039

de Waal Malefyt, R., Hans, Y., Roncarolo, M.-G., Spits, H., de Vries, J.E., 1992. Interleukin-10. Curr Opin Immunol 4, 314–320. https://doi.org/https://doi.org/10.1016/0952-7915(92)90082-P

Dinarello, C.A., 2007. Historical insights into cytokines. Eur J Immunol 37, S34–S45. https://doi.org/https://doi.org/10.1002/eji.200737772

Ensafi, A.A., 2019. An introduction to sensors and biosensors, in: Electrochemical Biosensors. Elsevier Inc., pp. 1–10. https://doi.org/10.1016/b978-0-12-816491-4.00001-2

Fame, R.M., Lehtinen, M.K., 2020. Emergence and developmental roles of the cerebrospinal fluid system. Dev Cell 52, 261–275.

Frías, I.A.M., Avelino, K.Y.P.S., Silva, R.R., Andrade, C.A.S., Oliveira, M.D.L., 2015. Trends in Biosensors for HPV: Identification and Diagnosis. J Sens 2015, 913640. https://doi.org/10.1155/2015/913640

Frias, I.A.M., Vega Gonzales Gil, L.H., Cordeiro, M.T., Oliveira, M.D.L., Andrade, C.A.S., 2021. Self-enriching electrospun biosensors for impedimetric sensing of zika virus. ACS Appl Mater Interfaces 14, 41–48.

Frutiger, A., Tanno, A., Hwu, S., Tiefenauer, R.F., Vörös, J., Nakatsuka, N., 2021. Nonspecific Binding—Fundamental Concepts and Consequences for Biosensing Applications. Chem Rev 121, 8095–8160. https://doi.org/10.1021/acs.chemrev.1c00044

Gao, F., Liu, C., Zhang, L., Liu, T., Wang, Z., Song, Z., Cai, H., Fang, Z., Chen, J., Wang, Junbo, Han, M., Wang, Jun, Lin, K., Wang, R., Li, M., Mei, Q., Ma, X., Liang, S., Gou, G., Xue, N., 2023. Wearable and flexible electrochemical sensors for sweat analysis: a review. Microsyst Nanoeng 9, 1. https://doi.org/10.1038/s41378-022-00443-6

Gwiazda, M., Kaushik, A., Chlanda, A., Kijeńska-Gawrońska, E., Jagiełło, J., Kowiorski, K., Lipińska, L., Święszkowski, W., Bhardwaj, S.K., 2022. A flexible immunosensor based on the electrochemically rGO with Au SAM using half-antibody for collagen type I sensing. Applied Surface Science Advances 9, 100258. https://doi.org/https://doi.org/10.1016/j.apsadv.2022.100258

Heeger, A.J., 2010. Semiconducting polymers: The Third Generation. Chem Soc Rev 39, 2354–2371. https://doi.org/10.1039/b914956m

Hilali, N., Ruankham, W., Aarón Morales Frías, I., Bellagambi, F.G., Hangouët, M., Martin, M., Bausells, J., Mohammadi, H., Amine, A., Zine, N., Errachid, A., 2023. Copper-free click chemistry assisted antibodies for immunodetection of interleukin-10 in saliva. Microchemical Journal 193, 108933. https://doi.org/https://doi.org/10.1016/j.microc.2023.108933

Jayasena, S.D., 1999. Aptamers: An Emerging Class of Molecules That Rival Antibodies in Diagnostics. Clin Chem 45, 1628–1650. https://doi.org/10.1093/clinchem/45.9.1628

Kim, Y., Prausnitz, M.R., 2021. Sensitive sensing of biomarkers in interstitial fluid. Nat Biomed Eng 5, 3–5.

Laterza, O.F., Hendrickson, R.C., Wagner, J.A., 2007. Molecular Biomarkers. Drug Inf J 41, 573–585. https://doi.org/10.1177/009286150704100504

Lee, M., Zine, N., Baraket, A., Zabala, M., Campabadal, F., Caruso, R., Trivella, M.G., Jaffrezic-Renault, N., Errachid, A., 2012. A novel biosensor based on hafnium oxide: Application for early stage detection of human interleukin-10. Sens Actuators B Chem 175, 201–207. https://doi.org/https://doi.org/10.1016/j.snb.2012.04.090

Levenson, V. V, Melnikov, A.A., 2013. Molecular biomarkers in 2013. Expert Rev Mol Diagn 13, 773–776. https://doi.org/10.1586/14737159.2013.850419

Liang, W., Liu, J., Yang, X., Zhang, Q., Yang, W., Zhang, H., Liu, L., 2020. Microfluidic-based cancer cell separation using active and passive mechanisms. Microfluid Nanofluidics 24, 26. https://doi.org/10.1007/s10404-020-2331-x

Lin, J., Peng, Z., Liu, Y., Ruiz-Zepeda, F., Ye, R., Samuel, E.L.G., Yacaman, M.J., Yakobson, B.I., Tour, J.M., 2014. Laser-induced porous graphene films from commercial polymers. Nat Commun 5, 5714. https://doi.org/10.1038/ncomms6714

Lin, T., Xu, Y., Zhao, A., He, W., Xiao, F., 2022. Flexible electrochemical sensors integrated with nanomaterials for in situ determination of small molecules in biological samples: A review. Anal Chim Acta 339461.

Liu, G., Lv, Z., Batool, S., Li, M., Zhao, P., Guo, L., Wang, Y., Zhou, Y., Han, S., 2023. Biocompatible Material-Based Flexible Biosensors: From Materials Design to Wearable/Implantable Devices and Integrated Sensing Systems. Small 2207879.

Liu, Q., Shi, W., Tian, L., Su, M., Jiang, M., Li, J., Gu, H., Yu, C., 2021. Preparation of nanostructured PDMS film as flexible immunosensor for cortisol analysis in human sweat. Anal Chim Acta 1184, 339010. https://doi.org/https://doi.org/10.1016/j.aca.2021.339010

Luo, X., Davis, J.J., 2013. Electrical biosensors and the label free detection of protein disease biomarkers. Chem Soc Rev 42, 5944–5962. https://doi.org/10.1039/C3CS60077G

Macdonald, J.R., Barsoukov, E., 2018. Impedance spectroscopy: theory, experiment, and applications. John Wiley & Sons.

Macdonald, J.R., Schoonman, J., Lehnen, A.P., 1981. Three dimensional perspective plotting and fitting of immittance data. Solid State Ion 5, 137–140.

Mathew, M., Radhakrishnan, S., Vaidyanathan, A., Chakraborty, B., Rout, C.S., 2021. Flexible and wearable electrochemical biosensors based on two-dimensional materials: Recent developments. Anal Bioanal Chem 413, 727–762. https://doi.org/10.1007/s00216-020-03002-y

Narayanan, K.B., Kim, H.D., Han, S.S., 2020. Biocompatibility and hemocompatibility of hydrothermally derived reduced graphene oxide using soluble starch as a reducing agent. Colloids Surf B Biointerfaces 185. https://doi.org/10.1016/j.colsurfb.2019.110579

Naresh, V., Lee, N., 2021. A review on biosensors and recent development of nanostructured materials-enabled biosensors. Sensors (Switzerland) 21, 1–35. https://doi.org/10.3390/s21041109

Nelis, J.L.D., Migliorelli, D., Jafari, S., Generelli, S., Lou-Franco, J., Salvador, J.P., Marco, M.P., Cao, C., Elliott, C.T., Campbell, K., 2020. The benefits of carbon black, gold and magnetic nanomaterials for point-of-harvest electrochemical quantification of domoic acid. Microchimica Acta 187, 164. https://doi.org/10.1007/s00604-020-4150-x

Oliveira, G.C.M. de, Carvalho, J.H. de S., Brazaca, L.C., Vieira, N.C.S., Janegitz, B.C., 2020. Flexible platinum electrodes as electrochemical sensor and immunosensor for Parkinson's disease biomarkers. Biosens Bioelectron 152, 112016. https://doi.org/https://doi.org/10.1016/j.bios.2020.112016

Pateraki, M., Fysarakis, K., Sakkalis, V., Spanoudakis, G., Varlamis, I., Maniadakis, M., Lourakis, M., Ioannidis, S., Cummins, N., Schuller, B., Loutsetis, E., Koutsouris, D., 2020. Biosensors and Internet of Things in smart healthcare applications: challenges and opportunities, Wearable and Implantable Medical Devices. https://doi.org/10.1016/b978-0-12-815369-7.00002-1

Potter, L.R., Yoder, A.R., Flora, D.R., Antos, L.K., Dickey, D.M., 2009. Natriuretic Peptides: Their Structures, Receptors, Physiologic Functions and Therapeutic Applications BT - cGMP: Generators, Effectors and Therapeutic Implications, in: Schmidt, H.H.H.W., Hofmann, F., Stasch, J.-P. (Eds.), . Springer Berlin Heidelberg, Berlin, Heidelberg, pp. 341–366. https://doi.org/10.1007/978-3-540-68964-5_15

Purohit, B., Vernekar, P.R., Shetti, N.P., Chandra, P., 2020. Biosensor nanoengineering: Design, operation, and implementation for biomolecular analysis. Sensors International 1, 100040. https://doi.org/10.1016/j.sintl.2020.100040

Ross, D., Heinemann, L., Chantelau, E.A., 1990. Short-term evaluation of an electro-chemical system (ExacTech^{TM}) for blood glucose monitoring. Diabetes Res Clin Pract 10, 281–285. https://doi.org/https://doi.org/10.1016/0168-8227(90)90071-Z

Rut'kov, E. V, Afanas'eva, E.Y., Gall, N.R., 2020. Graphene and graphite work function depending on layer number on Re. Diam Relat Mater 101, 107576. https://doi.org/https://doi.org/10.1016/j.diamond.2019.107576

Shkodra, B., Demelash Abera, B., Cantarella, G., Douaki, A., Avancini, E., Petti, L., Lugli, P., 2020. Flexible and Printed Electrochemical Immunosensor Coated with Oxygen Plasma Treated SWCNTs for Histamine Detection. Biosensors (Basel). https://doi.org/10.3390/bios10040035
Smith, C.G., Moser, T., Mouliere, F., Field-Rayner, J., Eldridge, M., Riediger, A.L., Chandrananda, D., Heider, K., Wan, J.C.M., Warren, A.Y., 2020. Comprehensive characterization of cell-free tumor DNA in plasma and urine of patients with renal tumors. Genome Med 12, 1–17.
Sreenilayam, S.P., Ahad, I.U., Nicolosi, V., Brabazon, D., 2021. Mxene materials based printed flexible devices for healthcare, biomedical and energy storage applications. Materials Today 43, 99–131.
Stein, A., Pache, R.A., Bernadó, P., Pons, M., Aloy, P., 2009. Dynamic interactions of proteins in complex networks: a more structured view. FEBS J 276, 5390–5405. https://doi.org/https://doi.org/10.1111/j.1742-4658.2009.07251.x
Strimbu, K., Tavel, J.A., 2010. What are biomarkers? Curr Opin HIV AIDS 5, 463.
Tebani, A., Gummesson, A., Zhong, W., Koistinen, I.S., Lakshmikanth, T., Olsson, L.M., Boulund, F., Neiman, M., Stenlund, H., Hellström, C., Karlsson, M.J., Arif, M., Dodig-Crnković, T., Mardinoglu, A., Lee, S., Zhang, C., Chen, Y., Olin, A., Mikes, J., Danielsson, H., von Feilitzen, K., Jansson, P.-A., Angerås, O., Huss, M., Kjellqvist, S., Odeberg, J., Edfors, F., Tremaroli, V., Forsström, B., Schwenk, J.M., Nilsson, P., Moritz, T., Bäckhed, F., Engstrand, L., Brodin, P., Bergström, G., Uhlen, M., Fagerberg, L., 2020. Integration of molecular profiles in a longitudinal wellness profiling cohort. Nat Commun 11, 4487. https://doi.org/10.1038/s41467-020-18148-7
Vasilijević, S., Boukraa, R., Battaglini, N., Piro, B., 2023. Graphene-based materials and their applications in electrolyte-gated transistors for sensing. Synth Met 295, 117355. https://doi.org/https://doi.org/10.1016/j.synthmet.2023.117355
Vozgirdaite, D., Ben Halima, H., Bellagambi, F.G., Alcacer, A., Palacio, F., Jaffrezic-Renault, N., Zine, N., Bausells, J., Elaissari, A., Errachid, A., 2021. Development of an ImmunoFET for Analysis of Tumour Necrosis Factor-α in Artificial Saliva: Application for Heart Failure Monitoring. Chemosensors 9, 26.
Wang, X., Chen, G., Zhang, K., Li, R., Jiang, Z., Zhou, H., Gan, J., He, M., 2023. Self-Healing Multimodal Flexible Optoelectronic Fiber Sensors. Chemistry of Materials 35, 1345–1354.
Watanabe, K., Miura, N., Taguchi, H., Komatsu, T., Nosaka, H., Okamoto, T., Watanabe, S., Takeya, J., 2022. Electrostatically-sprayed carbon electrodes for high performance organic complementary circuits. Sci Rep 12, 16009. https://doi.org/10.1038/s41598-022-19387-y
Wu, T., Wang, Q., Peng, X.Y., Guo, Y., 2021. Facile Synthesis of Gold/Graphene Nanocomposites for Simultaneous Determination of Sunset Yellow and Tartrazine in Soft Drinks. Electroanalysis. https://doi.org/10.1002/elan.202100464
Yan, S., Tan, S.H., Li, Y., Tang, S., Teo, A.J.T., Zhang, J., Zhao, Q., Yuan, D., Sluyter, R., Nguyen, N.-T., 2018. A portable, hand-powered microfluidic device for sorting of biological particles. Microfluid Nanofluidics 22, 1–10.
Ye, R., James, D.K., Tour, J.M., 2018. Laser-Induced Graphene. Acc Chem Res 51, 1609–1620. https://doi.org/10.1021/acs.accounts.8b00084
Zhang, F., Zhang, Z., Zhu, X., Kang, E.T., Neoh, K.G., 2008. Silk-functionalized titanium surfaces for enhancing osteoblast functions and reducing bacterial adhesion. Biomaterials 29, 4751–4759. https://doi.org/10.1016/j.biomaterials.2008.08.043
Zhang, Z., Zhao, H., Teng, Y., Chang, X., Xia, Q., Li, Z., Fang, J., Du, Z., Świerczek, K., 2018. Carbon-Sheathed MoS2 Nanothorns Epitaxially Grown on CNTs: Electrochemical Application for

Highly Stable and Ultrafast Lithium Storage. Adv Energy Mater 8, 1700174. https://doi.org/https://doi.org/10.1002/aenm.201700174
Zhu, P., Wang, L., 2017. Passive and active droplet generation with microfluidics: a review. Lab Chip 17, 34–75.

CHAPTER II

NON-COVALENT II–II FUNCTIONALIZED GRAPHENE FOAM FOR INTERLEUKIN 10 IMPEDIMETRIC DETECTION

SUMMARY OF CHAPTER II

In this work, the authors fabricated a 3-D printed microfluidic device featuring a clasping structure with resin-printed internal tubing which directs the fluids into the electrode chamber. The flow can be controlled by syringe pumps and therefore, the incubation, electrical measurements, and cleaning processes can be performed in an automated action. This microfluidic lab-on-chip device was designed for the impedimetric monitoring of IL-10 using graphene foam (GF) flexible electrodes. Graphene's conductivity and flexibility are attractive to offer simple single-use and reduced handling. Nevertheless, the main current strategy of oxidation of its carbon lattice to develop functional moieties for biomolecule immobilization cuts down its electronic conductivity potential. Therefore, we envisaged to maintain graphene's crystal structure by employing π–π non-covalent functionalization with pyrene carboxylic acid (PCA). Furthermore, monitoring Interleukin 10 (IL-10) is essential for understanding the vast responses of T-cells in cancer, auto- immunity, and internal homeostasis after physical stress.

Biosensors and Bioelectronics 222 (2023) 114954

Contents lists available at ScienceDirect

Biosensors and Bioelectronics

journal homepage: www.elsevier.com/locate/bios

Non-covalent π–π functionalized Gii-sense® graphene foam for interleukin 10 impedimetric detection

Isaac A. M. Frias [a], Nadia Zine [a], Monique Sigaud [a], Pablo Lozano-Sanchez [b], Marco Caffio [b], Abdelhamid Errachid [a,*]

[a] Université de Lyon, Institut des Sciences Analytiques, UMR 5280, CNRS, Université Lyon 1, ENS Lyon-5, Rue de La Doua, F-69100, Villeurbanne, France
[b] Integrated Graphene Ltd Eurohouse, Wellgreen Place Stirling, FK8 2DJ, Scottland, UK

ARTICLE INFO

Keywords:
Electrochemical impedance spectroscopy
Graphene foam
Chemisorption
Inter-leukin 10
Label-free detection
Pyrenes

ABSTRACT

Monitoring Interleukin 10 (IL-10) is essential for understanding the vast responses of T-cells in cancer, autoimmunity, and internal homeostasis after physical stress. However, current diagnostic methods are complex and more focused on medical screening rather than point-of-care monitoring. Biosensors based on graphene's conductivity and flexibility are attractive to offer simple single-use and reduced handling. However, oxidation of its carbon lattice to develop functional moieties for biomolecule immobilization cuts down its electronic conductivity potential. In this work, the authors present a microfluidic lab-on-chip device for simple impedimetric monitoring of IL-10 based on graphene foam (GF) flexible electrodes. Graphene's structure was maintained by employing π–π non-covalent functionalization with pyrene carboxylic acid (PCA). Impedimetric measurements could be performed in low ionic strength phosphate-buffered saline (LI-PBS). The PCA-antibody modification showed to endure the incubation, measurement, and washing processes performed in the microfluidic device. Electrode modification and measurements were characterized by, electrochemical impedance spectroscopy (EIS), contact angle, and scanning electron microscopy. From the contact angle results, we found that the wettability of the graphene surface increased gradually after each modification step. Detection measurements performed in the 3D-printed microfluidic device showed a linear response between 10 fg/mL to 100 fg/mL with a limit of detection (LOD) of 7.89 fg/mL in artificial saliva. With these features, the device was used to quantify IL-10 samples by the standard addition method for 10 fg and 50 fg with recoveries between 82% and 99%. Specificity was evaluated towards interleukin 6, TNF-α and bovine serum albumin.

1. Introduction

The coupling of aromatic molecules on graphene is used to prevent its stacking and agglomeration to improve its electrochemical storage (Bello et al., 2014). The pyrenil group is highly aromatic and its derivatives have been employed to provide functional groups for labeling and capturing small molecules (Chen et al., 2001). Chemisorbed aromatic compounds have shown excellent electron transfer from covalently bonded enzymes to carbon-based nanomaterials (Göbel and Lisdat, 2008). Their strong interaction is promising for the development of robust and sensitive biosensing devices and if needed the graphitic surface can be regenerated under ethyl acetate reflux conditions (Lu et al., 2010).

Electrochemical biosensors avail conductive or semiconductive materials with enhanced area-to-volume ratio to increase the number of anchoring sites and, therefore, the sensitivity. Carbon-based transducers have been studied for biological applications, and it is essential to highlight that carbon nanomaterials are more than suitable for developing flexible and stretchable transducers. Graphene is one of the most studied materials because its conductivity is higher than carbon nanotubes, and it can be used as an active channel, dielectric, or conductive electrode. However, it must be adapted by oxidation of the graphitic crystal, which produces defects mainly in the borders of the nanostructures; in this way, the electronic conduction is preserved to the detriment of the small number of anchoring sites. Further intense oxidation results in the creation of more functional groups, although the holes in the conductive crystal decrease the overall electronic conductivity.

Interleukin 10 (IL-10) is a 2α-helical cytokine homodimer. Considered a pleiotropic immunologic regulator, its functions encompass the

* Corresponding author.
E-mail address: abdelhamid.errachid@isa-lyon.fr (A. Errachid).

https://doi.org/10.1016/j.bios.2022.114954
Received 8 September 2022; Received in revised form 21 October 2022; Accepted 23 November 2022
Available online 30 November 2022

suppression and termination of inflammatory immune responses through the inhibition of monocyte and macrophage activation by increasing the production of anti-inflammatory factors, including soluble Tumour Necrosis Factor receptors (TNF-α) and IL-1RA. At the same time, it down-regulates the expression of MHC class II molecules (both constitutive and IFN-γ-induced), co-stimulatory molecule CD86, and adhesion molecule CD58. Considering its many biological interactions, IL-10 has significant clinical relevance to diseases such as heart disease (Lakoski et al., 2008), cancer (Mocellin et al., 2005), COVID-19 (Lindner et al., 2021), asthma (Hawrylowicz and O'garra, 2005), systemic lupus erythematosus (Beebe et al., 2002), psoriasis (Asadullah et al., 2004), inflammatory bowel disease (Glocker et al., 2009), rheumatoid arthritis (Zhang et al., 2011), and bacterial infections such as Tuberculosis (Wang et al., 2018).

IL-10 is usually assayed using commercially available ELISA kits (Sirilun et al., 2022), and its expression is evaluated through real-time PCR (Mar-Solís et al., 2021). The concentration of IL-10 in the salivary fluid of healthy individuals is usually found around 1.80 ± 0.81 pg/mL and monitoring gradual variations in its concentration is desirable to monitor the development of clinical disorders (Bertorello et al., 2004). Of note, intracellular levels of IL-10 are monitored by flow cytometry using labeled monoclonal antibodies (Fumeaux et al., 2004), and whole-cell fingerprints can be studied by MALDI-TOF MS (Daumas et al., 2018). All these techniques are reported as fast and straightforward; however, their sample preparation protocols are complex, not to mention the unique infrastructure and personnel requirements needed to perform them. For these reasons, biosensors are an excellent alternative for comprehensive and straightforward laboratory use. Adopting biosensors in clinical applications can shorten the response time of primary health services. However, the development of automated single-use biosensors is desired to offer widespread point-of-care monitoring.

In this work, the authors fabricated a 3-D printed microfluidic device featuring a clasping structure with resin-printed internal tubing which directs the fluids into the electrode chamber. The flow can be controlled by syringe pumps and therefore, the incubation, electrical measurements, and cleaning processes can be performed in an automated action. The π-π coupled carboxyl functional groups were activated through EDC-sulfoNHS chemistry to tether the antibodies. The electronic properties of the graphene promoted direct electron transfer from the capacitive double layer after the bio interaction event to the Gii-sense® graphene foam transducing layer. Because of this, the impedimetric measurements could be performed in LI-PBS, a suitable solution to work in clinical and home environments. Finally, this approach reduced handling, and simple measuring achieved detection limits in the order of femtograms per milliliter.

2. Experimental

2.1. Materials

Pyrene carboxylic acid (PCA), dichloromethane-H_2O saturated (DCM), tetrabutylammonium perchlorate (TBA), N-(3-Dimethylaminopropyl)-N′-ethyl carbodiimide hydrochloride (EDC), N-Hydroxysuccinimide (NHS), phosphate-buffered saline (PBS), 2-Morpholinoethanesulfonic Acid (MES) buffer and ethanolamine were purchased from Sigma Aldrich (USA). Polyclonal anti-IL-10 antibodies and IL-10 were obtained from R&D systems. Otherwise stated, all reagents were used without further modification. Standard solutions and buffers were prepared with deionized water (18.2 MΩ cm at 25 °C) obtained from an ELGA water purification system.

2.2. Modeling and fabrication of microfluidic device

The prototype modeling of the sensor's electrical reader was performed in ANSYS SpaceClaim software. After meticulous consideration, the fluid distribution system was integrated as internal microfluidic tubes, thus, providing the system with a cleanlier look. The diameter of the embedded channels is 1.6 mm and the total volume needed for the workflow including the electrode chamber is 268 μL ± 22 μL. The electrode chamber was made by including an O-ring to produce sufficient spacing for liquid replacement. The same lever that elevates the contact pins is the same lever that applies enough pressure to seal the O-ring over the sensing area. Connecting wires and tubing are inserted from below the lever and heading out through the back. The current prototype is qualified to perform accurate electrical measurements. Finally, the prototype was printed with clear V2 resin in a Form2 3-D printer from Formlabs (Somerville, Massachusetts, USA).

2.3. Fabrication of Gii-sense® graphene foam electrode

Gii-sense® GF electrodes were obtained from Integrated Graphene Ltd. Electrochemical. Briefly, graphene was embedded in polydimethylsiloxane, and the graphene foam of the electrode areas was directly grown on polyimide substrates by a catalyst-free method without the use of a transfer process. GF transducer displays a sensitivity of 0.0418 mV/kPa over a range from 1 to 50 kPa, and protective PDMS coating increases the durability of the sensors, keeping the voltage steady with no visible drop after numerous measurements (Douglas et al., 2021). The counter and working electrode are graphene foam in this device, and the reference electrode is solid contact Ag/AgCl. The working electrode diameter area is 4 mm with a 1 mm space between the counter electrode which surrounds it in a C format. To complete the system, the Ag/AgCl reference electrode is placed below the working electrode, and as a continuation of the counter electrode, maintaining 1 mm of separation (Fig. S1, in supplementary material).

2.4. Surface modification

2.4.1. Optimization of pyrene carboxylic acid deposition

Pyrene carboxylic acid solution was optimized by exploring its solubility in different organic solvents, namely dimethylformamide, dichloromethane, chloroform, and at 3 PCA concentration levels, low 5 mM, medium 10 mM, and high 20 mM, including 0.1M TBA as a phase transfer catalyst to increase solubility. The solutions were wise dropped over the working electrode 1 μL at a time until saturation. Even though PCA dissolves readily in DMF and dichloromethane, the solution spreads quickly over the adjacent electrodes, so DMF was selected. PCA concentration was selected at 10 mM since undissolved solids could be observed at 20 mM even after increasing TBA concentration. Along these lines, the surface of the working electrode was directly functionalized by dropping 5 μL of PCA solutions over the center of the working electrode. The chemisorption by π-complexation between PCA and graphene occurs at room temperature during a 30 min evaporation process. Afterward, the carboxyl groups were activated using 40 μL of a 0.4 M EDC/0.1 M Sulfo NHS (1:1) solution prepared in MES buffer (pH 6). Passed this time, the electrode was quickly washed, and 20 μL of a 10 μg/mL anti-IL-10 polyclonal antibody solution prepared in PBS (10 mM pH7.4) was dropped over the working electrode. After 1h immobilization, the electrode was washed with PBS buffer, and unspecific sites were blocked during a 30 min incubation with 10 μL 0.1 mM ethanolamine prepared in PBS buffer. Finally, this time the electrode was washed and submerged in PBS buffer at 4 °C until use.

2.5. Sample preparation

IL-10 samples were prepared in artificial saliva (Vozgirdaite et al., 2021) (AS) with 0.6 g/L of sodium phosphate dibasic (Na_2HPO_4, Sigma-Aldrich), 0.6 g/L sodium bicarbonate ($NaHCO_3$, Sigma-Aldrich), 0.6 g/L calcium chloride ($CaCl_2$, Sigma-Aldrich), 0.4 g/L potassium chloride (KCl, Sigma-Aldrich), 0.4 g/L sodium chloride (NaCl, Acros Organics), 4 g/L mucin (Sigma-Aldrich), and 4 g/L urea

(Sigma-Aldrich). Sodium hydroxide solution (NaOH, Sigma-Aldrich) was added to adjust pH to 7.4, and after preparation, aliquots were stored at −24 °C for later use.

2.6. Electrical characterization of the transducer and biosensor

Electrical measurements were performed using a Palm Sense 4 electrochemical workstation (Netherlands). Gii-sense® GF electrode was used as the working electrode (φ = 4 mm, WE) and counter electrode (CE), and printed silver/silver chloride as reference electrodes (RE). The Gii-sense®/PCA/AntiIL-10 biosensor was characterized by open circuit potential in PBS solution 0.1 mM and at different scan rates (from 0.01 to 0.1 v/s) by cyclic voltammetry in 5 mM $[Fe(CN)_6]^{3-}$/$[Fe(CN)_6^{4-}$ (1:1, v/v) prepared in PBS buffer as redox probe. IL-10 biorecognition was studied by EIS, and measurements were performed in PBS 0.1 mM as electrolyte solution at 4 °C inside a Faraday cage. PBS concentration was optimized to minimize the influence of ionic contributions in impedance spectroscopy. Spectra were obtained under sine wave potential with AC amplitude and DC set to 10 mV (DC set to the value of the open circuit potential) over a frequency range from 100 mHz to 100 kHz.

3. Results and discussion

3.1. Integrated microfluidic device and biosensor construction

In Fig. 1, we present the printed microfluidic system and SEM microscopy of the Gii-sense® GF, including a scheme of the modification of the transducer by chemisorption with pyrene carboxylic acid. The carboxyl groups of the pyrene carboxylic acid were availed to immobilize the anti-IL-10 antibodies. The modified transducer was used as an IL-10 biosensor. Oxidation of its Sp^2 carbon bonds will bring forward functional groups to the detriment of its conductive features (Morimoto et al., 2016). For these reasons, in this strategy, we seek incorporation in a polymeric blend which results in high porosity.

Graphene's electronic π clouds promote the stacking of PCA. Although they are not covalently attached, their electronic bands are connected and thus remain very sensitive to fluctuations in the overall electronic band structure around the immobilized antibodies (Mishyn and Hugo, 2022). In this sense, the π-π immobilized pyrene carboxylic acid molecules serve as an electronic wire that communicates the information of the immobilized antibodies. In Fig. S2 we present a comparison of the electrical responses of the electrode before and after functionalization with pyrene carboxylic acid. In general, we observed that the conductivity of the graphene foam is maintained, and we noticed a slight increase after coupling the pyrene carboxylic acid. Analyzers based on electrochemical impedance spectroscopy stand out because they can perform the analysis with high sensitivity without damaging the biological activity. In Fig. S3a (in supplementary material) we present the characterization of the open circuit potential of the Gii-sense®/Pyrene/anti-IL-10 biosensor in 0.1 mM PBS buffer. The stability between 10 mV and 11.5 mV is attained at 20 min. In addition, the variation of the scan rate from 0.01 V to 0.1 V in a scan from −0.2 V to 0.7 V in $[Fe(CN)_6]^{3-}$/$[Fe(CN)_6^{4-}$ (Fig. S3b) resulted in a linear tendency from 0.01 to 0.07 according to the equation, Anodic peak = 46.153x-15.522 with an $r^2 = 0.99$. Thus, the biosensor maintained its characteristics within the operating range.

During the fabrication of the biosensor, we studied the hydrophilicity of the surface of the transducer by contact angle measurements with water. Pictures taken during the experiment are shown in Fig. 2. Initially, the Gii-sense® transducer displays a hydrophobic characteristic with an angle of 149°, after π-complexation with PCA, a more hydrophilic feature was observed with an angle of 44°. After activation with EDC/NHS, the surface gains hydrophilicity according to an 18° angle. After anti-IL-10 immobilization, the contact angle attains its lowest point with a 4° angle, signaling that the surface was modified by the antibodies which also have more affinity towards water. Increases in contact angle evince that the sample can fully permeate the surface of the electrode.

In the next step, after blocking unspecific binding sites with ethanolamine, we observed an increase in the contact angle to 25°. This result demonstrates that the activated carboxyl groups that were not used by the antibody were blocked, and thus they should have limited activity toward aqueous solutions. Furthermore, because hydrophobic moieties repel water molecules, these molecules tend to move from the hydrophobic to the hydrophilic sites where the probe molecules are tethered, and therefore, the biosensor sensitivity is expected to be significantly increased (Kim et al., 2013). Finally, after a 250 fg/mL of IL-10 sample was incubated, the contact angle presented a value of 75°. Most likely, this effect is in direct relationship with the capture of IL-10 by the antibodies. Of note, in this study deionized water was used and therefore the proteins were distant from their optimal isoelectric point which is around pH 8.5. For this reason, we consider that since the anti-IL-10 modified substrate displayed the highest hydrophilicity, the

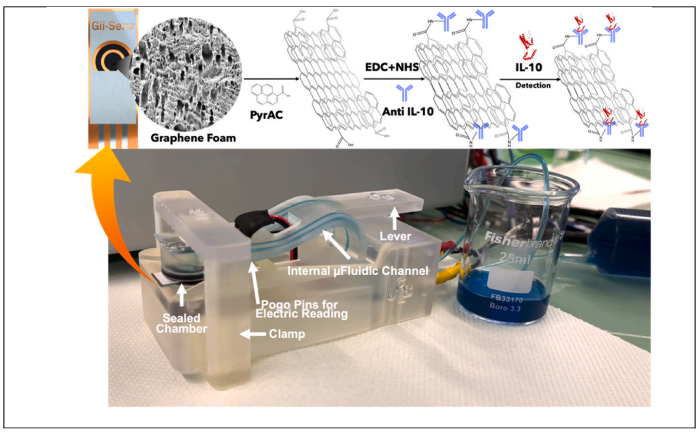

Fig. 1. Integrated Microfluidic System for Impedimetric Measurement. Scheme representation of the chemisorption of pyrene carboxylic acid in Gii-sense® GF for the immobilization of anti-IL-10 and IL-10 detection.

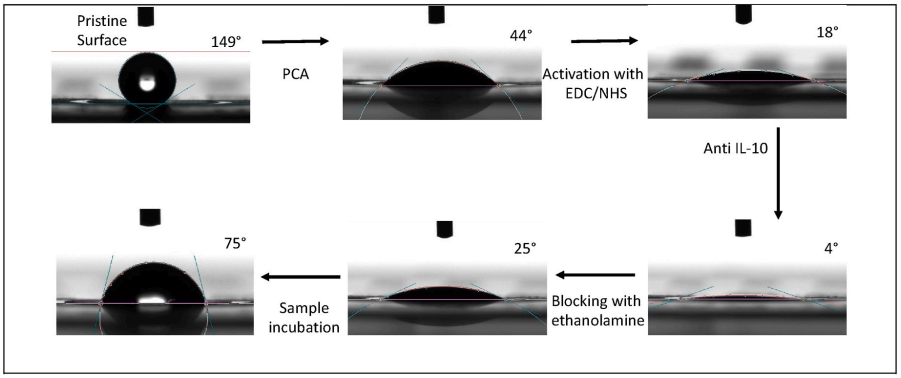

Fig. 2. Contact angle analyses of the transducer modification process and biosensing of a 250 fg/mL IL-10 sample.

wettable sites were then exhausted after interaction with IL-10. In addition, Fig. S4 presents SEM images at different stages of the modification of the transducer.

3.2. Impedimetric characterization of the sensor platform and analytical performance

The Gii-sense®/PCA/anti-IL-10 biosensor was tested with samples of artificial saliva (Vozgirdaite et al., 2021) containing different concentrations (from 10 to 100 fg/mL) of IL-10. The impedimetric responses are shown in Fig. 3a, and in the inset, we present the equivalent circuit used for the mathematical fitting of the impedimetric responses. Impedance spectroscopy allowed us to evaluate the charge behavior of the electrical double layer at the surface of the transducer as Nyquist plots were recorded with different concentrations of IL-10 present in artificial saliva samples. The impedimetric responses were mathematically fitted to an equivalent circuit consisting of the solution resistance (R_S) in series with a constant phase element (Q) in parallel with a charge transfer resistance (R_{CT}) and a Warburg impedance (W). The measurements are performed in 0.1 mM PBS buffer, therefore, the accumulation of IL-10 occurring at the electrode surface hinders electronic transfer and/or increases the impedance. For this reason, Q and R_{CT} depend on the dielectric and isolating aspects of the biosensor interface of the biosensor. These analytical signals and respective R_{CT} values are directly proportional to the concentration of the captured IL-10. The average values of the different elements and RSD (N = 3) of the equivalent circuit for 3 different electrodes are presented in Supplementary Information Table S1.

To compare the responses within different electrodes, R_{CT} values were normalized as $\%\Delta R_{CT} = \left|\frac{RCT_{(Gii-sense®\ /PCA/antiIL-10/IL-10)} - RCT_{(Gii-sense®\ /PCA/antiIL-10)}}{RCT_{(Gii-sense®\ /PCA/antiIL-10)}}\right| \times 100$. In Fig. 3b (black circles), we observe that ΔR_{CT} values increase gradually to the concentration of IL-10 present in the sample according to the equation $\%\Delta R_{CT} = 0.34$(IL-10 fg/mL)—0.059 with an $r^2 = 99\%$. From this calibration curve, the instrumental limit of detection was estimated as LOD = 3.33σ/S where σ = 0.81 is the standard deviation of the intercept of the regression line and S = 0.34 is the slope of the calibration curve, resulting in LOD = 7.9 fg/mL. In the same figure, in red points, we added the points corresponding to the analysis of three IL-10 samples prepared in artificial saliva. The three samples with concentrations of 0.2 pg/mL, 0.5 pg/mL and 0.7 pg/mL were diluted 10 times. After detection and

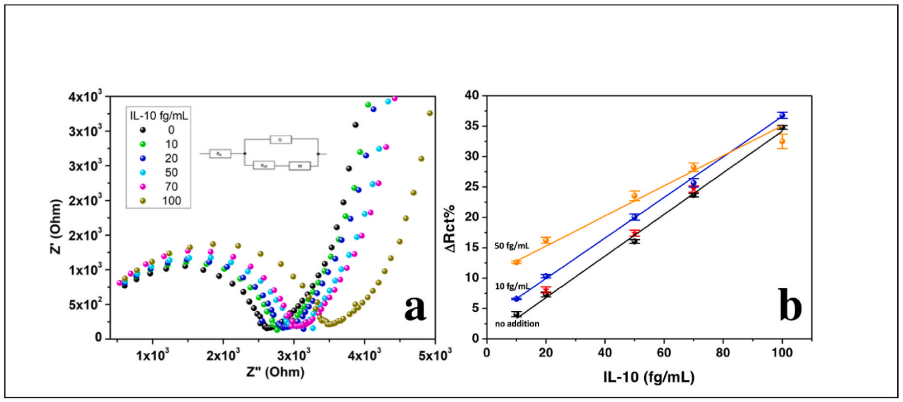

Fig. 3. a) Nyquist plot of the impedimetric responses of the Gii-sense®/PCA/anti-IL-10 biosensor after incubation in samples of artificial saliva containing different concentrations (from 10 to 100 fg/mL) of IL-10. In the inset, the equivalent circuit is used for the mathematical fitting of the impedimetric responses, b) the plot of R_{CT} vs the concentration of IL-10, in black circles, the calibration curve and red stars are those of samples both performed in artificial saliva. Blue and orange curves show the results using the standard addition method.

quantification performed with the Gii-sense®/PCA/anti-IL-10 biosensor, found concentrations were 23.7 fg/mL, 51.3 fg/mL and 72.6 fg/mL which after applying the dilution factor resulted in 0.23 ± 0.02 pg/mL, 0.51 ± 0.02 pg/mL and 0.72 ± 0.02 pg/mL respectively.

To evaluate the applicability of the modified biosensors as single-use devices, we tested artificial saliva samples containing an initial IL-10 concentration by the standard addition method to minimize the matrix effect. In these analyses, a calibration curve is performed, however, 50 μL of the sample are spiked at each point of the calibration curve. In Fig. 3b and Table S2, the results obtained with two samples at 10 and 50 fg/mL are shown. In blue circles, we observe the standard calibration curve for an initially added sample of 10 fg/mL of IL-10. The resultant equation of the calibration curve for this sample is $\%\Delta R_{CT} = 3.269 + 0.333$(IL-10 fg/mL) with an $r^2 = 98\%$. To calculate the concentration of the sample of the added volumes we solve the equation when $\%\Delta R_{CT} = 0$. As a result, we obtained a concentration of 9.8 ± 0.3 fg/mL. The result for the tested samples spiked with volumes of a 50 fg/mL sample is presented in orange circles. The equation for this sample is $\%\Delta R_{CT} = 10.316 + 0.247$(IL-10 fg/mL) with an $r^2 = 98\%$. For this sample, we calculated an initial concentration of, 41.7 ± 2 fg/mL.

In Fig. 4, we present the selectivity of the Gii-sense®/PCA/anti-IL-10 biosensor, evaluated towards potential protein interferences such as BSA, TNF-α, and IL-6. All the interferent samples were prepared in artificial saliva with three different concentrations: 20 fg/mL, 50 fg/mL, and 70 fg/mL to be in similar concentrations of the analyte. Analyzing these interferents, we observed that the variation of $\%\Delta R_{CT}$ was negligible in all of them. The Gii-sense®/PCA/anti-IL-10 biosensor was specific only for IL-10. No tendency was observed in the graphics, and a correlation between the interference concentration and the signal couldn't be established.

Previously, our group has immobilized specific antibodies to detect different cytokines of clinical interest in complex samples. For instance, silicon nitride was used for TNF-α detection within the range of 1 pg/mL to 30 pg/mL (Bahri et al., 2020). Another group reported the impedimetric detection of IL-6 from 0.01 to 100 fg/mL based on AuNPs-decorated horizontally aligned single-walled carbon nanotubes arrayed on a SiO2/Si substrate (Yang et al., 2013). However, the use of complex materials and fabrication techniques might difficult the reproducibility of the devices. In addition to the fact that using ferri/-ferrocyanide redox probe could challenge waste disposal management in healthcare services. Our diagnostic system stands out because the combination of the electrical properties of the graphene foam and their preservation after functionalization with pyrene carboxylic acid allows the detection of very low protein concentrations while employing LI-PBS (Chu et al., 2017).

In Table 1 we compare the analytical performance of the fabricated Gii-sense®/PCA/anti-IL-10 biosensor with previously published interleukin-10 sensors. The detection of IL-10 has gained attention in the last 10 years, and many EIS-based biosensors have been developed for its quantification in non-complex matrices. The published methods highlight pg/mL detection range and many attractive state-of-the-art materials were developed for this goal. For instance, solid substrates such as hafnium oxide and silicon/gold chips have attained limits of detection of 100 fg/mL (Lee et al., 2012). On the other hand, materials that can be deposited over flexible substrates such as polypyrrole have shown limits of detection close to 350 fg/mL (Nessark et al., 2020). Of note, previous publications have performed their measurements in non-complex matrices, so their applicability is still to be established.

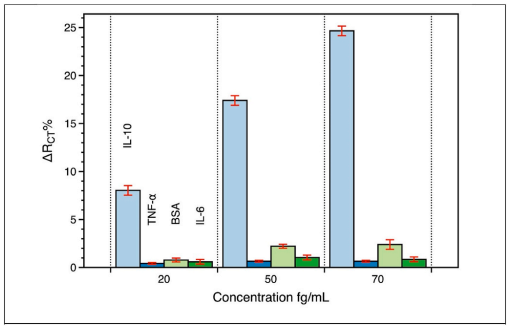

Fig. 4. $\Delta R_{CT}\%$ values were obtained for different interferents (TNF-α, BSA and IL-6) compared to IL-10.

In this work, highly conductive Gii-sense® GF was chosen because of its conductive features, while its porosity heightens the area-to-volume ratio. No oxidation was needed to develop functional groups. The π-π immobilization of pyrene-carboxylic acid in graphene was already attempted for electrochemical storage applications. In addition, because this foam prevents graphene flakes from restacking, its conductivity is perfectly maintained (Bello et al., 2014). With these characteristics, the Gii-sense®/PCA/anti-IL-10 biosensor presented in this work displayed a linear detection range from 10 to 100 fg/mL and a limit of detection of 7.89 fg/mL. Furthermore, the biosensor showed good performance towards artificial saliva samples, and good selectivity towards IL-10 compared to interferents such as TNF-α, BSA, and IL-6, not to mention the mucin and urea present in the preparation of artificial saliva.

4. Conclusion

A specific biosensor for IL-10 based on a Gii-sense® graphene foam transducer was developed. The electronic features of graphene were maintained because its functionalization was achieved without oxidation by the π-complexation of pyrene carboxylic acid. As a result, impedimetric measurements of low protein concentrations were performed in LI-PBS, a suitable solution for clinical environments and with easier disposal compared to common redox-probe solutions. Interleukin-10 was quantified in a complex matrix, artificial saliva, in the range from 10 to 100 fg/mL with an instrumental limit of detection of 7.89 fg/mL. Samples tested by the method of standard addition showed that the system possesses good detection capabilities for single-use applications. The biosensor was selective towards IL-10 regarding interferent biomolecules that can be present in real saliva samples such as TNF-α and interleukin-6. GF functionalized by chemisorption of PCA is a transducer with an enhanced capacitance that can be used to develop cheap cost and well-performing electrochemical biosensors for point-of-care applications.

Funding sources

The authors acknowledge the financial support of the POC4allergies project (Grant Agreement No. 768686), which received funding from ERA PerMed ERA-NET, and the financial support from Bionanosens project (Grant agreement No. 951887), which received funding from the European Union's Horizon 2020.

CRediT authorship contribution statement

Isaac A. M. Frias: contributed to, Methodology, Validation, Formal analysis, Investigation, Data curation, Writing – original draft. **Nadia Zine:** contributed to, Supervision, Writing – review & editing. **Monique Sigaud:** contributed to, Writing – review & editing, reviewing. **Pablo Lozano-Sanchez:** contributed to the, Methodology, Investigation. **Marco Caffio:** contributed to, Writing – review & editing. **Abdelhamid Errachid :** contributed to, Supervision, Writing – review & editing, Funding acquisition.

Table 1
Comparison of the analytical performance of Gii-sense®/PCA/anti-IL-10 sensor with previously published interleukin 10 sensors.

Method	Transducer	IL-10 immobilization	Electrolyte	Sample matrix	Linearity (fg/mL)	LOD (fg/mL)	Ref
EIS	hafnium oxide (HfO2)	MAb Anti-IL-10 TESUD[a]	PBS 10 mM	PBS 10 mM	100–20.000	100	Lee et al. (2012)
EIS	Gold on a silicon chip	MAb Anti-IL-10 CMA[b]	$[Fe(CN)_6]^{-3}$/$[Fe(CN)_6]^{-4}$	PBS 10 mM	1.000–15.000	100	Baraket et al. (2017)
EIS	PPy/Si_3N_4[c]	MAb Anti-IL-10 CMA	PBS 10 mM	PBS 10 mM	1.000–100.000	347	Nessark et al. (2020)
EIS	Gii-sense®	PAb Anti-IL-10/Pyrene carboxylic acid	PBS 0.1 mM	Artificial Saliva	10–100	7.89	This work

[a] 11-(triethoxysilyl) undecanal
[b] 4-carboxymethyl aryl diazonium.
[c] Polypyrrole modified silicon nitride.

Declaration of competing interest

The authors declare that they have no known competing financial interests or personal relationships that could have appeared to influence the work reported in this paper.

Data availability

No data was used for the research described in the article.

Appendix A. Supplementary data

Supplementary data to this article can be found online at https://doi.org/10.1016/j.bios.2022.114954.

References

Asadullah, K., Sabat, R., Friedrich, M., Volk, H.D., Sterry, W., 2004. Curr. Drug Targets - Inflamm. Allergy 3, 185–192.
Bahri, M., Baraket, A., Zine, N., ben Ali, M., Bausells, J., Errachid, A., 2020. Talanta 209, 120501.
Baraket, A., Lee, M., Zine, N., Sigaud, M., Bausells, J., Errachid, A., 2017. Biosens. Bioelectron. 93, 170–175.
Beebe, A.M., Cua, D.J., de Waal Malefyt, R., 2002. Cytokine Growth Factor Rev. 13, 403–412.
Bello, A., Fabiane, M., Momodu, D.Y., Khamlich, S., Dangbegnon, J.K., Manyala, N., 2014. J. Solid State Electrochem. 18, 2359–2365.
Bertorello, R., Cordone, M.P., Contini, P., Rossi, P., Indiveri, F., Puppo, F., Cordone, G., 2004. Clin. Exp. Med. 4, 148–151.
Chen, R.J., Zhang, Y., Wang, D., Dai, H., 2001. 123, 3838–3839.
Chu, C.-H., et al., 2017. Sci. Rep. 7, 5256.
Daumas, A., Alingrin, J., Ouedraogo, R., Villani, P., Leone, M., Mege, J.-L., 2018. BMC Infect. Dis. 18, 355.
Douglas, C.I., Nuñez, C.G., Gibson, D., Caffio, M., 2021. 13th Spanish Conference on Electron Devices (CDE), pp. 141–144.
Fumeaux, T., Dufour, J., Stern, S., Pugin, J., 2004. Intensive Care Med. 30, 2028–2037.
Glocker, E.-O., Kotlarz, D., Boztug, K., Gertz, E.M., Schäffer, A.A., Noyan, F., Perro, M., Diestelhorst, J., Allroth, A., Murugan, D., 2009. N. Engl. J. Med. 361, 2033–2045.
Göbel, G., Lisdat, F., 2008. Electrochem. Commun. 10, 1691–1694.
Hawrylowicz, C.M., O'garra, A., 2005. Nat. Rev. Immunol. 5, 271–283.
Kim, J.-Y., Choi, K., Moon, D.-I., Ahn, J.-H., Park, T.J., Lee, S.Y., Choi, Y.-K., 2013. Biosens. Bioelectron. 41, 867–870.
Lakoski, S.G., Liu, Y., Brosnihan, K.B., Herrington, D.M., 2008. Atherosclerosis 197, 443–447.
Lee, M., Zine, N., Baraket, A., Zabala, M., Campabadal, F., Caruso, R., Trivella, M.G., Jaffrezic-Renault, N., Errachid, A., 2012. Sens. Actuators, B 175, 201–207.
Lindner, H.A., Velásquez, S.Y., Thiel, M., Kirschning, T., 2021. Front. Immunol. 12, 602130.
Lu, F., Wang, X., Meziani, M.J., Cao, L., Tian, L., Bloodgood, M.A., Robinson, J., Sun, Y.-P., 2010. Langmuir 26, 7561–7564.
Mar-Solís, L.M., et al., 2021. Medicina 57 (11), 1138.
Mishyn, V., Hugo, et al., 2022. Sensors & Diagnostics 1, 235–244.
Mocellin, S., Marincola, F.M., Young, H.A., 2005. J. Leukoc. Biol. 78, 1043–1051.
Morimoto, N., Kubo, T., Nishina, Y., 2016. Sci. Rep. 6, 21715.
Nessark, F., Eissa, M., Baraket, A., Zine, N., Nessark, B., Zouaoui, A., Bausells, J., Errachid, A., 2020. –1806. Electroanalysis 32, 1795.
Sirilun, S., Chaiyasut, C., Pattananandecha, T., Apichai, S., Sirithunyalug, J., Sirithunyalug, B., Saenjum, C., 2022. Antioxidants 11 (2), 305.
Vozgirdaite, D., ben Halima, H., Bellagambi, F.G., Alcacer, A., Palacio, F., Jaffrezic-Renault, N., Zine, N., Bausells, J., Elaissari, A., Errachid, A., 2021. Chemosensors 9, 26.
Wang, X., Wu, Y., Jiao, J., Huang, Q., 2018. Tuberculosis 108, 118–123.
Yang, T., Wang, S., Jin, H., Bao, W., Huang, S., Wang, J., 2013. Sens. Actuators, B 178, 310–315.
Zhang, J., Zhang, Y., Jin, J., Li, M., Xie, K., Wen, C., Cheng, R., Chen, C., Lu, J., 2011. Cytokine 56, 351–355.

Non-Covalent π–π Functionalized Gii-sense® Graphene Foam for Interleukin 10

Impedimetric Detection

[1]*Isaac A. M. Frias,* [1]*Nadia Zine,* [1]*Monique Sigaud,* [2]*Pablo Lozano-Sánchez,* [2]*Marco Caffio,*

[1*]*Abdelhamid Errachid.*

[1] Universite Claude Bernard Lyon1, ISA, UMR 5280 CNRS, 5 rue de la Doua 69100 Villeurbanne FRANCE
[2] Integrated Graphene Ltd Eurohouse, Wellgreen Place Stirling, FK8 2DJ, Scottland, UK.

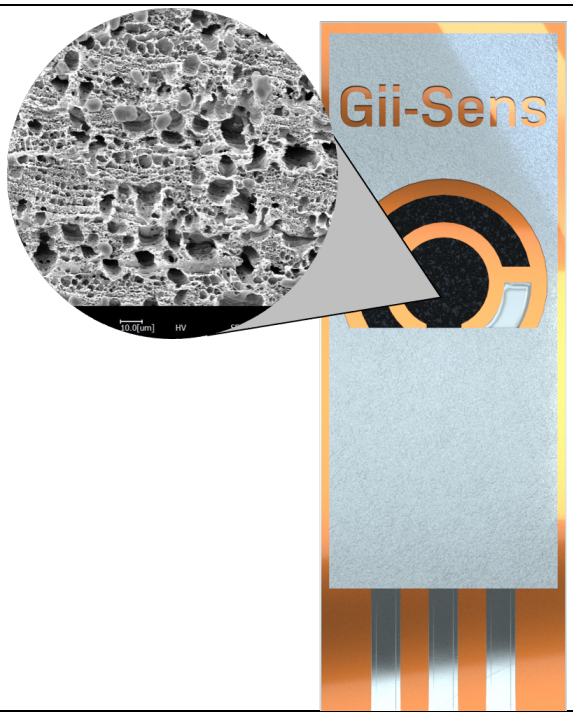

Figure S1. Gii-Sense graphene foam sensor.

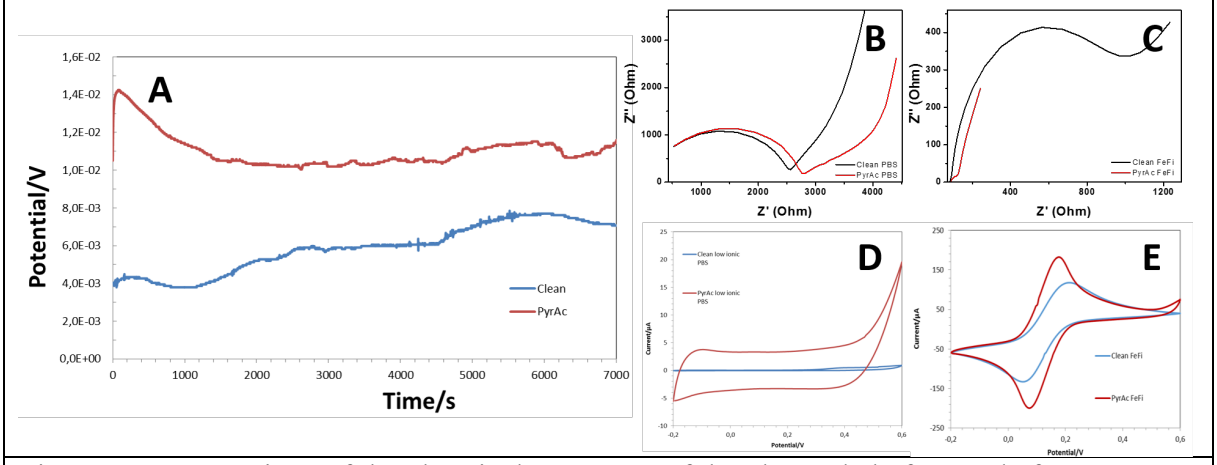

Figure S2. Comparison of the electrical responses of the electrode before and after functionalization with pyrene acetic acid. A) open circuit potential in low ionic strength phosphate-buffered saline. B) EIS and D) CV performed in low ionic strength phosphate-buffered saline. C) EIS and E) CV performed in $[Fe(CN)_6]^{3-}/[Fe(CN)_6^{4-}$.

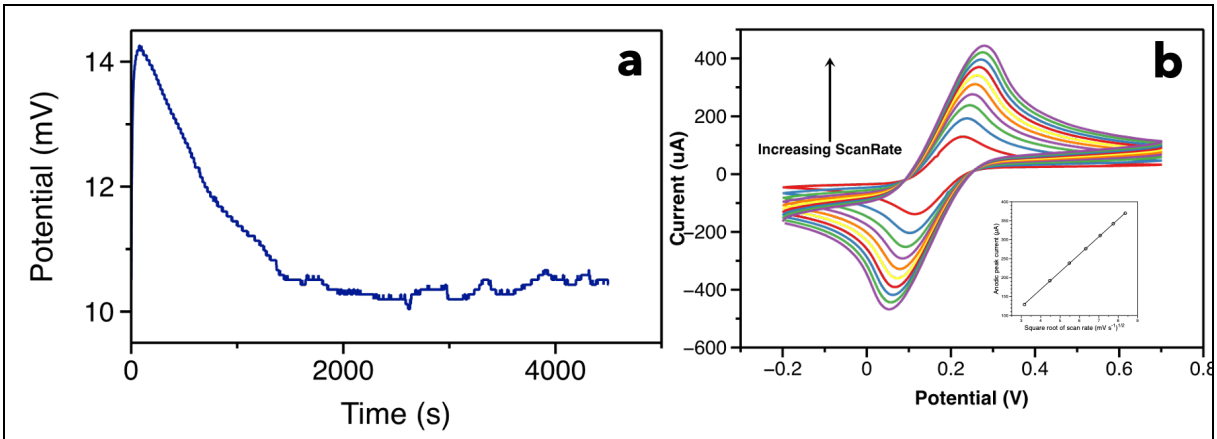

Figure S3. a) open circuit potential characterization in low-ionic strength phosphate-buffered saline and b) scan rate characterization from 0.01 V to 0.1 V by cyclic voltammetry characterization in $[Fe(CN)_6]^{3-}/[Fe(CN)_6^{4-}$ of the Gii-sense®/Pyrene/anti IL-10 biosensor.

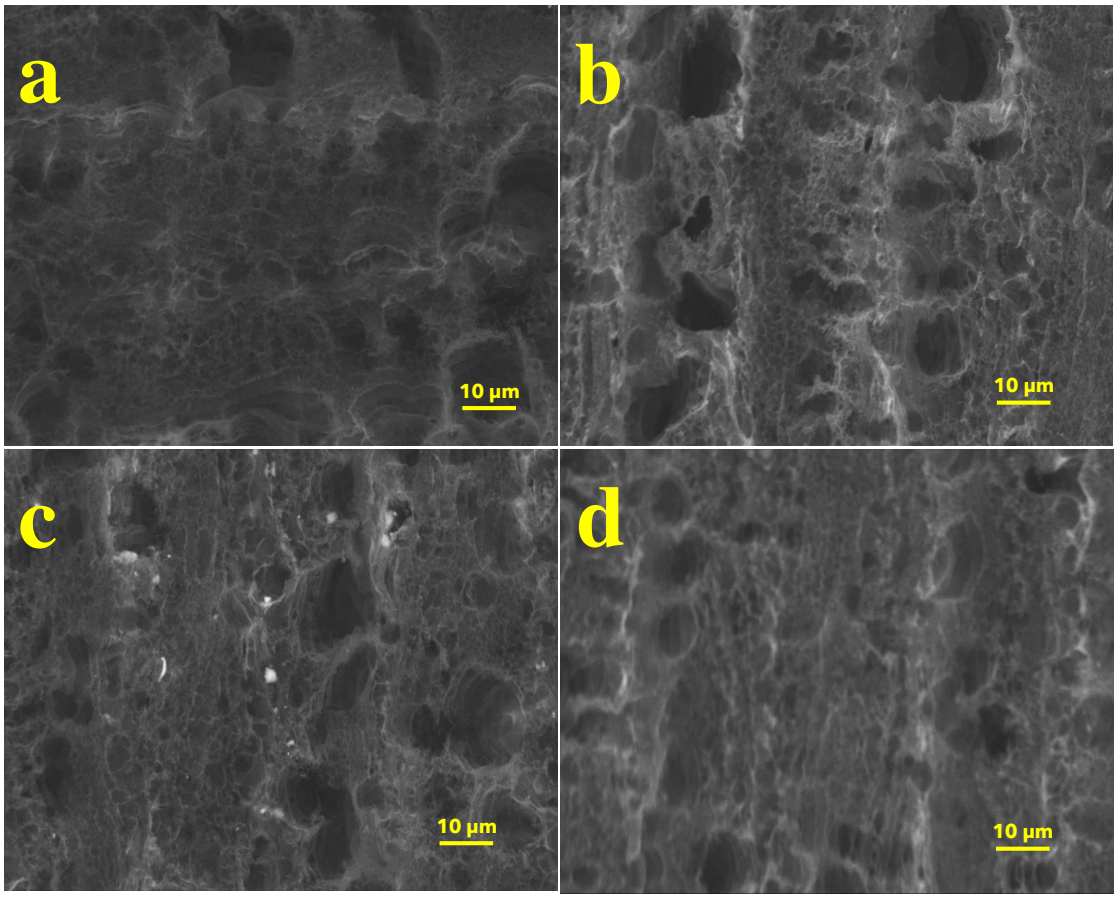

Figure S4. SEM characterization of the surface of the Gii-sense® GF transducer, a) after PCA, b) after antibody immobilization, c) after IL-10 capture, and d) analysis of a negative IL-6 sample.

In Fig. S4a, the Gii-sense® GF transducer modified with PCA is shown as a porous substrate with homogeneous contrast as the electron beam is conducted relentlessly over the surface. In Fig. S4b, after antibody immobilization, light contrast can be perceived on the surface of the substrate because of the presence of the insulant macromolecule (Saito et al., 2003). After detecting the 250 fg/mL IL-10 sample, it can be observed in Fig. S4c that mass agglomerations of light contrast are now present over the surface. Of note, these agglomerations were not found over the surface of the biosensor exposed to IL-6 samples (Fig. S4d), therefore, most likely they proceed from the captured IL-10 material.

Table S1. Electrical parameters and RSD obtained by the fitting of the electrochemical data with the equivalent circuit (mean value obtained from 3 electrodes).

CALIBRATION CURVE						
	Rs	CPE	N	RCT	W	ΔR_{CT}

GII-SENSE® /PCA/ANTI-IL-10/	79.78	1.10E-08	0.84232	2603	841	--
10 fg/mL	84.92	1.08E-08	0.84382	2709	959	4.07±0.2
20 fg/mL	98.80	1.02E-08	0.84682	2793	1524	7.30±0.2
50 fg/mL	97.31	1.11E-08	0.84005	3020	1170	16.03±0.1
70 fg/mL	95.82	7.84E-09	0.83528	3218	1061	23.64±0.1
100 fg/mL	91.74	1.34E-08	0.82593	3508	543	34.77±0.1
IL-10 SAMPLES						
	Rs	CPE	N	RCT	W	ΔR_{CT}
20 fg/mL	96.71	1.02E-08	0.84654	2812	1401	8.03±0.5
50 fg/mL	98.91	1.11E-08	0.84058	3056	1323	17.39±0.5
70 fg/mL	97.63	1.06E-08	0.84302	3244	1043	24.64±0.5
INTERFERENCES						
TNF-α						
	Rs	CPE	N	RCT	W	ΔR_{CT}
20 fg/mL	91.30	9.17E-09	0.85834	2592	10785	-0.41±0.1
50 fg/mL	98.21	9.78E-09	0.8538	2586	14708	-0.64±0.1
70 fg/mL	97.85	1.08E-08	0.84537	2586	17530	-0.64±0.1
BSA						
	Rs	CPE	N	RCT	W	ΔR_{CT}
20 fg/mL	94.53	1.11E-08	0.84139	2583	597	-0.77±0.2
50 fg/mL	93.21	1.14E-08	0.83979	2545	820	-2.21±0.2
70 fg/mL	95.36	1.10E-08	0.84235	2541	751	-2.39±0.5
IL-6						
	Rs	CPE	N	RCT	W	ΔR_{CT}
20 fg/mL	98.77	9.81E-09	0.85405	2587	94700	-0.58±0.2
50 fg/mL	92.44	9.79E-09	0.85402	2576	99055	-1.03±0.2
70 fg/mL	96.52	9.60E-09	0.85413	2581	12201	-0.84±0.2

Table S2. Results of the Standard additional method

Addition	*Added volume at each point of the curve*	*Equation*	*Calculated concentration when $\Delta R_{CT}=0$*	r^2	*Calculated concentration when $\Delta R_{CT}=0$*
10 fg/mL	50 µL	$\%\Delta R_{CT}=3.269+0.333$(IL-10 fg/mL)	9.8± 0.3 fg/mL	98	9.8± 0.3 fg/mL
50 fg/mL	50 µL	$\%\Delta R_{CT}=10.316+0.247$(IL-10 fg/mL)	41.7 ± 2 fg/mL	98	41.7 ± 2 fg/mL

CHAPTER III

IMPEDIMETRIC NT-proBNP POCT APTASENSOR BASED ON SCREEN PRINTED CARBON ELECTODES AND MALEIMIDE CLICK CHEMISTRY.

SUMMARY OF CHAPTER III

In this work, the authors envisaged to fabricate an impedimetric point of care test (POCT) for heart failure biomarkers that can be used with a cellphone. An updated minimal size 3-D printed microfluidic device was constructed featuring a screw fastener structure with internal tubing printed in resin to direct the fluids into the electrode chamber. The minimal flow of 100 μL are controlled by syringe pumps and, the incubation, electrical measurements, and cleaning processes can be performed in an automated action. This microfluidic lab-on-chip device was designed for the impedimetric monitoring of NT-proBNP using screen printed carbon flexible electrodes. Although graphene foam-based electrodes have shown to be very good electrochemical transducers in comparison to regular screen-printed carbon electrodes (SPCE), their price is more elevated. For this reason, in this strategy we designed outstanding chemistry and biological strategies to enhance their response. Briefly, pyrene maleimide was covalently tethered to the substrate through π-π interactions and the maleimide group was used for the specific click chemistry with thiolated oligonucleotide aptamers specific for NT-proBNP.

Abstract

Despite the enormous amount of transduction methods in which biosensors are being developed, producing effective devices at very low cost and with efficient waste management could lead to their popularization as monitoring devices. Carbon-based electrodes are very appreciated because of their flexibility. Although the conductivity of graphene is higher, so is their cost in comparison to regular screen-printed carbon electrodes (SPCE). In this work, the authors combined outstanding click chemistry and biological strategies to enhance SPCEs electrochemical response inside a miniaturized microfluidic system in which, incubation, measurement and washing occur with limited manipulation and automated operation. Availing SPCEs derivative structures with carbon sp^2-hybridized honeycomb lattice and other polycyclic aromatic hydrocarbons, pyrene maleimide was chemisorbed by π-complexation to the substrate through π-π interactions. The bioelectronic properties and stability of the biorecognition layer were enhanced by the click reaction between maleimide and thiolated oligonucleotide aptamers specific for NT-proBNP, which is a heart failure-specific cardiac biomarker with high diagnostic and prognostic relevancy.

Keywords: Screen printed carbon electrodes; Aptamers; Microfluidics; Click chemistry; pi interactions.

1. Introduction

Conductive carbon-based inks are among the most interesting materials for biodetection applications. Their high electrical conductivity, chemical stability, mechanical strength, biocompatibility, and biodegradability are some of their alluring properties that can be availed to improve the signal processing of electrochemical biosensors. In addition, their easy dispersion allows to ink-coat the most diverse substrates such as recyclable and biodegradable polymers. Differently from pure carbon nanomaterials (graphene, carbon nanotubes, etc.), the price of carbon-inks decreases according to the different proportions of metal particles, carbon compounds, polymer binders, plasticizers, dispersion agents and solvents used during their fabrication. For this reason, SPCE can be used as single use electrodes and are suitable for monitoring chronical clinical conditions such as heart failure.

Heart failure (HF) is a condition that causes the muscle in the heart wall to slowly weaken and enlarge, preventing the heart from pumping enough blood. The lack of fast diagnostic alternatives leads to undertreatment, delayed diagnosis and possible permanent heart damage; HF is commonly misdiagnosed based on clinical signs and symptoms alone (M. et al., 2019). However, many biomarkers are produced following the progression of the disease. In this context, NT-proBNP is a specific cardiac inflammation biomarker with high diagnostic and prognostic relevancy toward HF. Its testing is limited to conventional techniques such as echocardiography and laboratory immunoassays like ELISA(Chen et al., 2022), which complexity and response times are incompatible with the primary health care level. The age-related cut-points for NT-proBNP in serum are correlated with HF severity. For instance, 450 pg/mL for ages <50 y.o.; 900 pg/mL for ages 50–75 y.o. and 1800 pg/mL for ages >75 y.o. (Januzzi et al., 2006). Alternative detection and quantification methodologies have been developed, including, mass spectroscopy (Nougué et al., 2023), lateral flow immunoassays (Wilkins et al., 2018) and biosensors (optical, electrochemical, and potentiometric) (Alawieh et al., 2019). Most of them are designed for bench working with bulky and expensive detection instruments which need to be miniaturized to allow their use in POCTs. In addition, some of the limitations of current biosensors is their size, cost, speed, and sensitivity requirements. On the other hand, as promising as they are, electrochemical biosensors sensitivity is impacted by nonspecific binding, the ionic strength of the sampling solution, limited electron transfer and the double layer capacitance at the electrode surface.

To overcome these drawbacks, in this work, we applied outstanding chemistry and biological strategies to enhance the response of a single use NT-proBNP aptasensor developed

in a screen-printed carbon electrode (SPCE). Within the composition of this carbon material, there is an unknown proportion of conductive graphite derivative structures with sp^2-hybridized honeycomb lattice and other polycyclic aromatic hydrocarbons (Liao et al., 2019). As a result, pyrene maleimide is chemisorbed to the substrate through π-π interactions and the maleimide group is available for specific click chemistry with sulfhydryl groups at pH between 6.5-7.5. For this reason, the aptamers were synthesized with a thiol group modification in the 5' side. Having assembled these bioreceptors directly over the surface in a single step, we avoided further modifications on the sp^2 carbon lattice. In addition to the known high chemical stability of the aptamers, oligonucleotides in general are known to mediate fast electron transfer by migration of charge over long distances (Lisdat et al., 1999). It is with these two strategies that commercial SCPE were enhanced to detect NT-proBNP at the femtogram range in complex serum samples.

2. Materials and methods.

2.1.Reagents.

Pyrene maleimide (Py-mal), dimethylformamide (DMF), absolute ethanol and dithiothreitol (DTT) were bought from Fischer Scientific (France). Bovine serum albumin (BSA), human serum, potassium ferrocyanide and potassium ferricyanide were bought from Sigma Aldrich (France). NT-proBNP, TNFα, BNP and IL-6 were bought from HyTest (Finland).

The aptamer used in this research (properties MW:22579.3 g/mol, Tm 89.2°C.) was screened from a library of random nucleic acid molecules by microfluidic "systematic evolution of ligands by exponential enrichment" (SELEX) process which involves an iterative process of nucleic acid binding, separation, and amplification. The oligonucleotide sequence "5' GGC AGG AAG ACA AAC AGG TCG TAG TGG AAA CTG TCC ACC GTA GAC CGG TTA TCT AGT GGT CTG TGG TGC TGT" was selected in conditions resembling real serum samples which include the presence of BSA and other proteins (Sinha et al., 2018). Therefore, its use in this aptasensor is guaranteed to have reduced interference when analyzing real samples. The sequence was synthetized by Mycrosynth France with a 5' thiol modification.

2.2.Electrical characterization of the aptasensing platform

In this research, we used a portable Sensit Smart (PalmSens) potentiostat with a compliance range from 100nA to 1mA, EIS frequency ranges from 0.016 Hz to 200 kHz and a full DC-potential range from -1.7 V to +2 V. On the regular conditions of analysis, this portable

potentiostat requires a great amount of the time to perform a full analysis including cyclic voltammetry (CV) and impedance spectroscopy (EIS), i.e. more than 1h per analysis. Considering this extensive time, the analysis conditions were optimized to only perform EIS analysis in repetition until equilibrium in a current range from 100 µA to 1 mA, applying a DC potential of 0.2 V and a AC potential of 0.1V, measuring 40 frequency points within the range of 5 Hz to 10 000 Hz. Working in these parameters the stabilization and complete analysis occurs in 15 min. All measurements were performed triplicate in ferri/ferrocyanide $Fe(CN)^{3-}$ /$Fe(CN)^{4-}$ redox couple

2.3.Fabrication of the 3D printed microfluidic box.

The prototype modeling of the sensor's electrical reader was performed in ANSYS Space Claim software. After meticulous consideration a prototype was developed considering the dimensions of the miniaturized electrode. Internal microfluidic tubing was integrated, and the liquid chamber was created by means of the spacing of an O-ring. All parts needed for the miniaturized model were 3D printed in the Micro & Nanobiotechnology Lab (ISA, Lyon). The system was proved for leaks and suitable touching towards the contacts of the sensor. Finally, the prototype was printed with clear V2 resin in a Form2 3-D printer from Formlabs (Somerville, Massachusetts, USA).

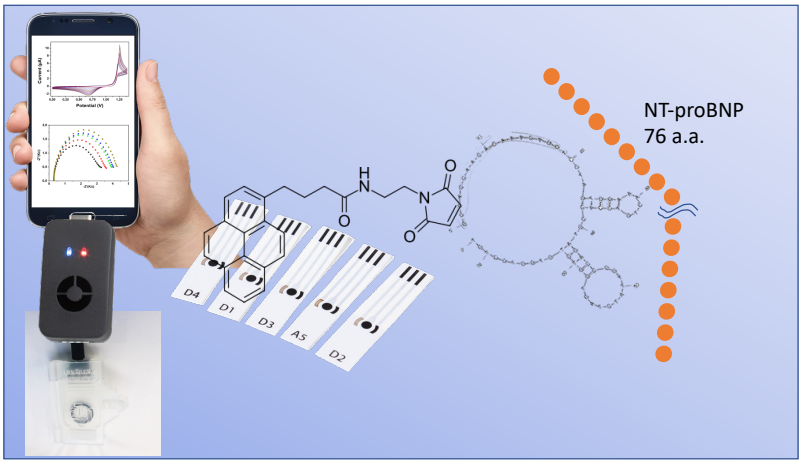

Figure 1. Graphical abstract

3. Results and Discussion

3.1.Fabrication of the sensing platform.

In this work, ItalSens carbon screen printed electrodes were used. In Fig.2 we show cyclic voltammetry characterization performed in H_2SO_4 demonstrating that, when scanning to more positive potentials over 1.2V, a reduction peak occurs around 1.1 V. The proposed mechanism

for this effect is associated to the creation of activated sulfur trioxide through protonation during the oxidation of H_2SO_4.

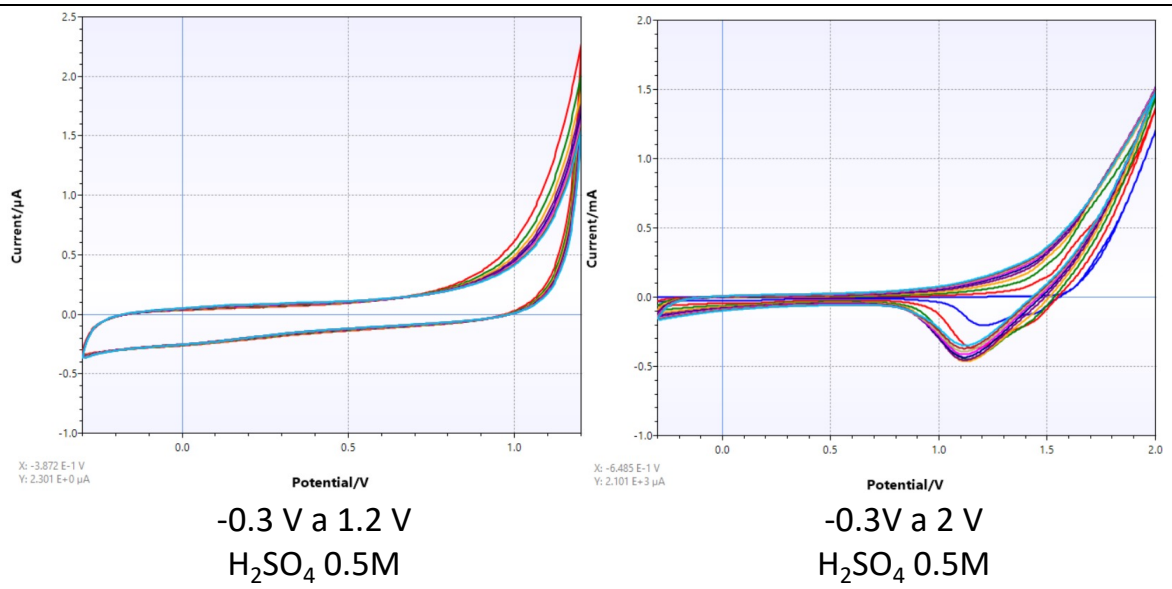

Figure 2. Changes in reduction peak of italsense SPE immersed in 0.5 H_2SO_4, after applying different voltage ranges by CV

In Fig.3A. we show the cyclic voltammetry spectra of the he activation of the silver reference electrode and cleaning of the working electrode, performing 15 cycles from 0 to 1.5V using a 0.5M KCl and 0.5M H_2SO_4 solutions. We observe that the addition of KCl stabililzes the reduction peak at 70 mV, which increases negatively after each cycle. This result indicates that the carbon structures used in this electrode were oxidized forms of sp^2 hexagonal carbon network decorated with carboxyl, hydroxyl, or epoxy functional groups. At each cycle, the increase of negative current of this peak is attributed to the reduction of these functional groups. This result is in accordance with the results of other groups searching to promote the electrochemical reduction of graphene oxide films (Ramesha and Sampath, 2009). In addition, our result also shows that in this process, the reduced oxidized carbon lattice does not get re-oxidized within the applied potential and therefore, this reduction is an irreversible process. After the reduction of the carbon surface, the π cloud can resume to hover over longer distances and therefore conductivity is increased. At the same time, endorsing this electronic behavior is key for the chemisorption of Py-mal.

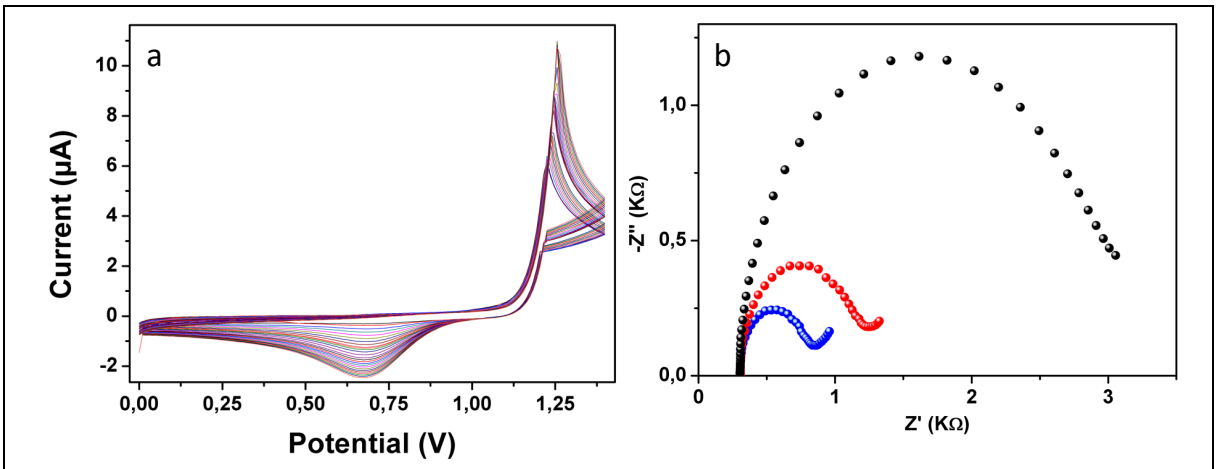

Figure 3. a) Cyclic voltammogram of the conditioning processes of the SPC electrode, b) Impedance spectroscopy of platform fabrication at different stages, clean (blue), pyrene maleimide (red), aptamer (black).

Subsequently, a 12.18 M Py-mal solution was prepared in dimethyl formamide (DMF) to promote better solubility. From there, an ethanolic solution at 0.14M was prepared, and 0.5µL of that solution was dropped over the SPCE working electrode. Immediately after evaporation, to remove non bounded Py-mal, the electrodes were washed with ethanol, then DI water, finally dried with compressed air.

To form the aptamer's 3D structure, 1 µL of a 10µM DTT solution was added to 5 µL of a 100 nM aptamer solution to reduce disulfide bounds of the thiolated aptamers. The aliquot was heated at 95 °C for 5 min and cooled immediately to 4 °C for 10 min. At this point, 4 µL were dropped over the working electrode and incubated at 4 °C overnight. Finally, the biosensor was washed with PBS buffer 10 mM and characterized. In Fig. 3B. we show the impedimetric characterization depicted as Nyquist plots where, the smallest blue semicircle is the initial clean electrode, the next red one is the response of the electrode after the chemisorption of Py-mal and finally the biggest semicircle is the response after click immobilization of the aptamer. We observe the impedance increases because of the shielding effect these molecules exert over the carbon surface.

3.2.Evaluation of serum samples with the aptasensor.

The impedimetric responses of the aptasensor were evaluated through the mathematical fitting of the Nyquist plots to Randal's equivalent circuit, consisting of solution resistance (R_S), and constant phase element (CPE) in parallel with charge transfer resistance (R_{CT}). Because of the setting parameters chosen for these analyses, Warburg resistance was not considered. As

the aptasensor captures NT-proBNP, its accumulation shields the surface from the redox probe, thus increasing impedance. Dielectric and isolating aspects of the aptasensor's interface are reflected in RCT, which increases proportionally to the concentration of captured NT-proBNP.

Using conventional ELISA kit approved for diagnostic use in Europe, human serum samples were validated in the range of 85-5424 pg/mL with a limit of detection provided by the manufacturer LOD=25.4 pg/mL (Bellagambi et al., 2021). Initially, the aptasensor was tested with NT-proBNP solutions (1, 10, 25, 50, 100 and 200 fg/mL) prepared in PBS to create a calibration curve. The response of the aptasensor showed a determination coefficient of 0.99 following the equation y = 0.072x + 3.4763, standard deviation of the intercept of the regression line (σ=0.237) and slope (S= 0.072). The instrumental limit of detection was estimated as LOD= 3.33 σ/S= 10.95 fg/mL. Before analyzing NT-proBNP in human serum samples, the matrix effect was evaluated by exposing the aptasensor to different concentrations of pure human serum samples (0.001%, 0.01%, 0.05% and 0.1%) . In Fig. 4 we show the ΔR_{CT} values obtained with each dilution.

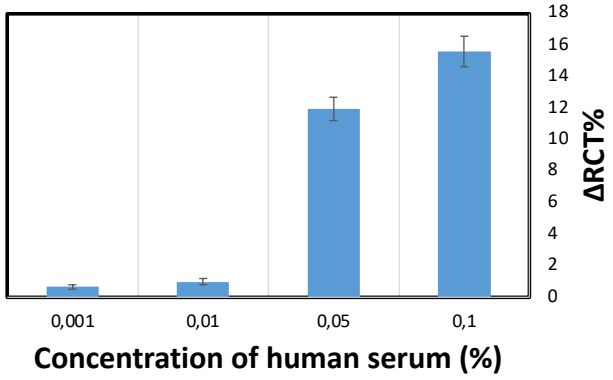

Figure 4. Matrix effect of human serum over the aptasensor at different dilution factors.

The optimal dilution range of plasma for application of the test with minimal interference from the matrix was chosen to be 0.01% or 1:10 000 dilution. Considering HF NT-proBNP cut-offs, a sample containing around 1800 pg/mL is expected to be diluted at the fg/mL range. To evaluate the performance of the aptasensors as single-use devices, we tested a human serum sample containing a known initial NT-proBNP concentration of 80 fg/mL (after dilution factor 800 pg/mL) by the standard addition method. In Fig. 5a we show the Nyquist plots obtained with the aptasensor after analyzing increasing concentrations of NT-proBNP in human serum following standard addition method. The calibration curve was prepared in human serum 0.01%, however,50 µL of the known sample were spiked at each point of the calibration curve.

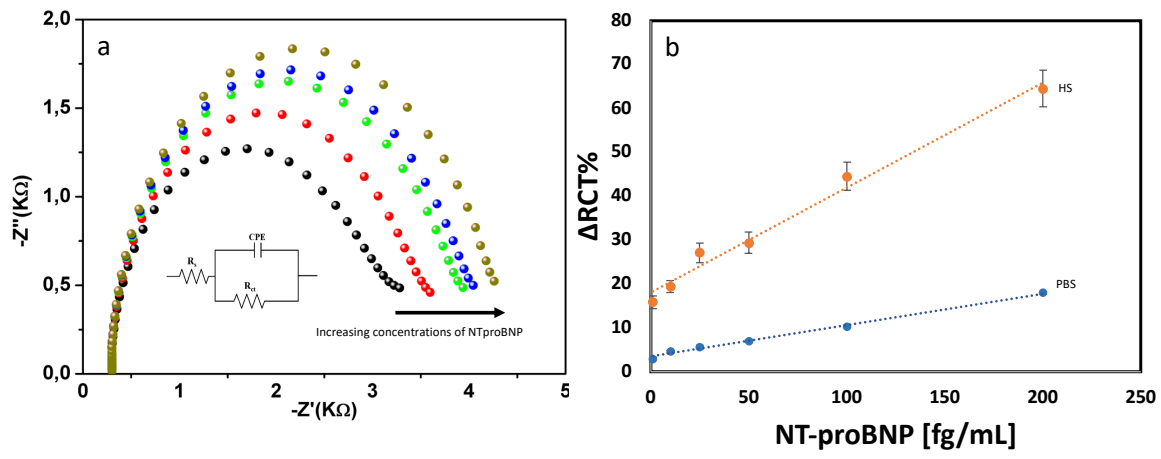

Figure 5. Impedimetric responses of the biosensor after being exposed to samples containing different concentrations of NT-proBNP.

Fitting these Nyquist plots with the equivalent circuit we obtained the results shown in Table 1 with the average values of the different elements and RSD (N = 3). The normalization of R_{CT} was calculated $\%\Delta R_{CT} = \left|\frac{RCT_{(\text{Carbon /Pymal/aptamer/NTproBNP})} - RCT_{(\text{Carbon /Pymal/aptamer})}}{RCT_{(\text{Carbon /Pymal/aptamer})}}\right| \times 100$, and these values were plotted in Fig. 5b.

Table 1. Results obtained with the aptasensor at different concentrations of NT-proBNP human serum samples for the different electric elements of Randal's equivalent circuit.

fg/mL	Rs	CPE-Q	CPE-n	R_{CT}	ΔR_{CT}%	E(±)
ini	281,3	4,43E-07	0,965	2931		
1	280,4	4,42E-07	0,969	3397	15,8	1,5
10	280,4	4,42E-07	0,970	3501	19,4	1,3
25	280,1	4,40E-07	0,970	3726	27,1	2,3
50	280,2	4,39E-07	0,969	3793	29,4	2,4
100	280,2	4,39E-07	0,969	4237	44,5	3,2
200	280,1	4,39E-07	0,966	4822	64,5	4,2

As a result, the standard addition method calibration curve was fitted by the equation $\Delta R_{CT}\% = 0.239$ (NTproBNP fg/mL) + 18.108, $R^2 = 0{:}98$. To calculate the concentration of the known sample, we solve the equation when $\%\Delta R_{CT} = 0$. As a result, we obtained a concentration of 75.7 ± 3.1 fg/mL or 757 pg/mL after applying the dilution factor with a recovery of 95%.

In Fig. 6a, we present the selectivity of the aptasensor evaluated towards potential protein interferences such as TNF-α, BNP and IL-6. All the interferent samples were prepared in human serum 0.01% at 10, 50 and 120 fg/mL (100, 500 and 1200 pg/mL after dilution factor) to be in similar concentrations of the analyte. Analyzing these interferents, we didn't observe interferent

interaction or tendencies of adsorption over the surface. Highlighting the specific nature of the aptamer used in this research, which was selected with SELEX from biomolecules likely found in human serum. In addition, in Fig 6b we show the stability results of the aptasensors, prepared, dried, and kept at 4°C during 5, 7 and 15 days. The ΔR_{CT}% of the response to a single 50 fg/mL NTproBNP sample in human serum 0.01% was very similar during the tested time, thus suggesting high accuracy and robustness of the fabricated aptasensor.

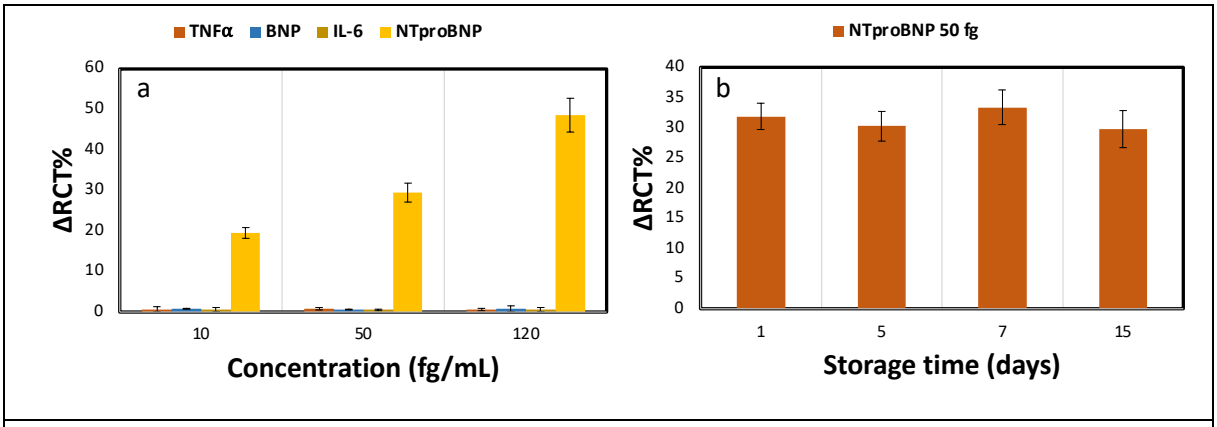

Figure 6. a)ΔR_{CT}% values obtained for different interferents at 10, 50 and 120 fg/mL (TNF-α, BNP and IL-6) compared to NTproBNP detection, and b) stability test of the aptasensor after storage at 4°C for 5, 7 and 15 days.

The development of aptasensors for heart failure biomarkers has been gaining attention over the last 5 years. In this manner, the interest is to advance in the direction of monitoring aptasensors that are robust, accurate and specific, in addition to decomplicated handling, cheap and single use. We notice that screen printed electrodes accomplish some of these requirements, however, gold screen printed electrodes require their modification with nanoparticles to increase their specific area. For instance, gold SPE were modified with reduced graphene oxide and polymers to attach azide-modified aptamers onto the surface by cupper-catalyzed click chemistry (Grabowska et al., 2018). With this strategy, the authors managed to analyze human serum samples in the range of clinical interest by differential pulse voltammetry (DPV) in Ferro/Ferri cyanide redox probe. Another outstanding research reported the grafting of azide-modified aptamers by UV photochemistry over a graphene field effect transistor (Nekrasov et al., 2022). They attained a linear range 0.1 – 1000 pg/mL in spiked PBS samples. Recently, our group reported feasibility of using NT-proBNP aptamer over a silicon-based gold surface microchip as a promising point-of-care tool for noninvasive saliva testing (Ruankham et al.,

2023). Subsequently, we reported the development of a microfluidic lab-on-chip device for simple impedimetric electrochemical monitoring of IL-10. We managed to size π-π interactions to modify graphene foam electrodes with carboxyl groups without altering its crystalline structure. Because of its high conductivity the impedimetric measurements could be performed in low ionic strength PBS (Frias et al., 2023). However, we are aware that cost might be a critical factor for the implementation of monitoring devices at the primary health care level or even for prescription-free monitoring devices. For that reason, in this work, we transformed the most common screen-printed carbon electrodes, by reducing their carbonic Sp^2 structures to condition the π-π chemisorption of a pyrene-maleimide molecule for direct click chemistry immobilization of thiol-modified aptamers; the 5' thiol modification is one of the most common types of modification that oligonucleotides can undergo. Although the electronic properties of SPCE are not as elevated as pure graphene electrodes, with these exceptional chemical and biological approaches, we attained a linear range from 0.001-0.2 in human serum samples diluted 1:10 000, which after applying the dilution factor covers the clinical range of interest from 100 to 2000 pg/mL.

Table 2.

Technique	Biorecognition	Platform	Sample	Linear range (pg/mL)	LOD (pg/mL)	Ref
DPV	NH_2BNP aptamer Cu(I)-catalyzed click chemistry	Gold SPE/polyethyleneimine/reduced graphene oxide	Human serum	1 – 1000	0.9	(Grabowska et al., 2018)
EIS	NH_2-terminated aptamer EDC/NHS	Au microchip	Artificial saliva	0.005 – 1.0	0.005	(Ruankham et al., 2023)
Voltammetry	Azide-Aptamer UVphotochemistry	Graphene field effect transistor	PBS	0.1 – 1000	0.01	(Nekrasov et al., 2022)
EIS	Thiol-Aptamer π-π Maleimide click chemistry	Screen printed carbon electrode	Human serum	0.001-0.2	0.01	This work

4. Conclusions

In this work we fabricated a minimal area microfluidic box, where sample incubation, measurement and flushing away can be performed in automation with the help of syringe pumps. The conductivity of regular screen-printed carbon electrodes was enhanced by reducing Sp^2 carbon structure lattices and at the same time, the restored π electron cloud was seized for

the chemisorption of pyrene maleimide through π-π interactions. The maleimide chemistry allowed us to bind covalently a very selective NTproBNP thiolated aptamer over the surface. Our results show that this aptasensor integrated microfluidic device is promising for the fast measurement of NTproBNP in human serum samples and can be used with a portable potentiostat and a cellphone.

5. Bibliography

Alawieh, H., El Chemaly, T., Alam, S., Khraiche, M., 2019. Towards Point-of-Care Heart Failure Diagnostic Platforms: BNP and NT-proBNP Biosensors. Sensors. https://doi.org/10.3390/s19225003

Bellagambi, F.G., Petersen, C., Salvo, P., Ghimenti, S., Franzini, M., Biagini, D., Hangouët, M., Trivella, M.G., Di Francesco, F., Paolicchi, A., Errachid, A., Fuoco, R., Lomonaco, T., 2021. Determination and stability of N-terminal pro-brain natriuretic peptide in saliva samples for monitoring heart failure. Sci Rep 11, 13088. https://doi.org/10.1038/s41598-021-92488-2

Chen, S., Zhou, Y., Wu, X., Shi, S., Wu, H., Li, P., 2022. The Value of Echocardiography Combined with NT-pro BNP Level in Assessment and Prognosis of Diastolic Heart Failure. Comput Math Methods Med 2022.

Frias, I.A.M., Zine, N., Sigaud, M., Lozano-Sanchez, P., Caffio, M., Errachid, A., 2023. Non-covalent π–π functionalized Gii-sense® graphene foam for interleukin 10 impedimetric detection. Biosens Bioelectron 222, 114954.

Grabowska, I., Sharma, N., Vasilescu, A., Iancu, M., Badea, G., Boukherroub, R., Ogale, S., Szunerits, S., 2018. Electrochemical Aptamer-Based Biosensors for the Detection of Cardiac Biomarkers. ACS Omega 3, 12010–12018. https://doi.org/10.1021/acsomega.8b01558

Januzzi, J.L., van Kimmenade, R., Lainchbury, J., Bayes-Genis, A., Ordonez-Llanos, J., Santalo-Bel, M., Pinto, Y.M., Richards, M., 2006. NT-proBNP testing for diagnosis and short-term prognosis in acute destabilized heart failure: an international pooled analysis of 1256 patients: the International Collaborative of NT-proBNP Study. Eur Heart J 27, 330–337.

Liao, Y., Zhang, R., Wang, H., Ye, S., Zhou, Y., Ma, T., Zhu, J., Pfefferle, L.D., Qian, J., 2019. Highly conductive carbon-based aqueous inks toward electroluminescent devices, printed capacitive sensors and flexible wearable electronics. RSC Adv 9, 15184–15189. https://doi.org/10.1039/c9ra01721f

Lisdat, F., Ge, B., Scheller, F.W., 1999. Oligonucleotide-modified electrodes for fast electron transfer to cytochrome c. Electrochem commun 1, 65–68. https://doi.org/https://doi.org/10.1016/S1388-2481(99)00006-5

M., W.R., Sabahat, B., Thibaud, D., M., E.P., H., F.R., M., F.N., Mariana, G., Laura, O., Claudio, R., Pablo, G.-P., 2019. Screening for Transthyretin Amyloid Cardiomyopathy in Everyday Practice. JACC Heart Fail 7, 709–716. https://doi.org/10.1016/j.jchf.2019.04.010

Nekrasov, N., Kudriavtseva, A., Orlov, A. V, Gadjanski, I., Nikitin, P.I., Bobrinetskiy, I., Knežević, N.Ž., 2022. One-Step Photochemical Immobilization of Aptamer on Graphene for Label-Free Detection of NT-proBNP. Biosensors (Basel). https://doi.org/10.3390/bios12121071

Nougué, H., Michel, T., Picard, F., Lassus, J., Sadoune, M., Laribi, S., Cohen-Solal, A., Logeart, D., Launay, J.-M., Vodovar, N., 2023. Deconvolution of BNP and NT-proBNP immunoreactivities by mass spectrometry in heart failure and sacubitril/valsartan treatment. Clin Chem 69, 350–362.

Ramesha, G.K., Sampath, S., 2009. Electrochemical Reduction of Oriented Graphene Oxide Films: An in Situ Raman Spectroelectrochemical Study. The Journal of Physical Chemistry C 113, 7985–7989. https://doi.org/10.1021/jp811377n

Ruankham, W., Frías, I.A.M., Phopin, K., Tantimongcolwat, T., Bausells, J., Zine, N., Errachid, A., 2023. One-step impedimetric NT-proBNP aptasensor targeting cardiac insufficiency in artificial saliva. Talanta 124280.

Sinha, A., Gopinathan, P., Chung, Y.-D., Lin, H.-Y., Li, K.-H., Ma, H.-P., Huang, P.-C., Shiesh, S.-C., Lee, G.-B., 2018. An integrated microfluidic platform to perform uninterrupted SELEX cycles to screen affinity reagents specific to cardiovascular biomarkers. Biosens Bioelectron 122, 104–112. https://doi.org/https://doi.org/10.1016/j.bios.2018.09.040

Wilkins, M.D., Turner, B.L., Rivera, K.R., Menegatti, S., Daniele, M., 2018. Quantum dot enabled lateral flow immunoassay for detection of cardiac biomarker NT-proBNP. Sens Biosensing Res 21, 46–53.

CHAPTER IV

IMPEDIMETRIC DETECTION OF ANTI- β 2-GLYCOPROTEIN I IGG ANTIBODIES.

SUMMARY OF CHAPTER IV

In this work, we developed a silicon-based four-plotted gold electrode biosensor for the detection and quantification of antiphospholipid antibodies. We continued to explore the maleimide click chemistry reaction as a quick and efficient method to develop biorecognition layers in biosensors. The electrografting of diazonium salts over gold has been reported to be fragile or weak because the electrocatalytic reaction stops after the first cycle. Here we report optimized parameters allowing the monolayer deposition of amino phenyl maleimide, a known click chemistry molecule specific to bond thiol groups.

ABSTRACT

The antiphospholipid syndrome is defined by the presence of antiphospholipid antibodies in serum. β2GPI protein is the main antigenic target for anti-phospholipid antibodies, and anti-β2GPI is the aPL associated with the lowest live birth rate and increased incidence of preeclampsia, intrauterine growth restriction, and stillbirth, compared with the presence of anticardiolipin antibodies or lupus anticoagulant alone

In this work we used IIa-8.0-2x, an epitope peptide selected by our group for its highest aPL-binding activity, however its spatial orientation is critical to maintain its biological activity. To overcome this challenge, we optimized the electro grafting of phenyl maleimide. The highly oriented film allowed us to immobilize IIa-8.0-2x in an orientation that our group describes as "seaweed in the current", by sizing by click chemistry the epitope peptide from the N-terminal side that features a cysteine residue. The biosensor showed linearity from 1 to 12 pg/mL with a limit of detection of 0.8 pg/mL (N=4). When analyzing serum sample from patients, we obtained a recovery of 112 % (10.7 ng/mL). These promising results indicate that the biosensor here presented could help in the fast quantification and monitoring of patient's serum samples. . In our results from the very first cycle, we observe irreversible reduction peaks at -0.84, related to the electrocatalytic reaction, and at -1 V related to the non-catalyzed reaction after the grafting of the monolayer is established. Therefore

Keywords: Electrochemical Impedance Spectroscopy; Click Chemistry; β2GP1; ApoH; Pregnancy complications; Label-free Detection; Electrografting.

1. INTRODUCTION

The antiphospholipid syndrome (APS) is defined by the presence of antiphospholipid antibodies (aPL) and clinical manifestations such as recurrent thromboembolic events and/or pregnancy complications (Miyakis et al., 2006). If no other autoimmune disease is simultaneously present, the syndrome is classified as primary APS otherwise, when other autoimmune disorders are present such as systemic lupus erythematosus (SLE), it is named secondary or associated APS (Alijotas-Reig et al., 2022). β2GPI is a protein of 43 kDa considered to be the main antigenic target for aPL. Following the updated Sapporo criteria, the anti-β2 glycoprotein I (anti-β2GPI) antibody has been added to the laboratory criteria which already include the presence of anticardiolipin (aCL) and/or lupus anticoagulant (LAC), on two or more occasions at least 12 weeks apart, for the diagnostic of APS (Saccone et al., 2017). However, anti-β2GPI is the one associated with the lowest live birth rate and highest incidence of preeclampsia, intrauterine growth restriction, and stillbirth, compared with the presence of anticardiolipin antibodies or lupus anticoagulant alone. Along these lines, a monitoring diagnostic appears very useful for close surveillance and tailored treatment before, during, and after pregnancy to optimize maternal and fetal pregnancy outcomes (Gerardi et al., 2018).

Electrografting of diazonium salts on gold electrodes has been studied for several phenylamine-derived molecules with different functional groups (Hetemi et al., 2020). The electrografting of amino phenyl maleimide (APM) has been performed in the past from solutions prepared in organic solvents onto glassy carbon, pyrolytic graphite, and gold surfaces. However, a problem frequently reported when electrografting aryl diazonium salts is that the grafting in gold surfaces is considered rather weak because the electrocatalytic reaction stops after the first cycle (Harper et al., 2008). In this work, electrografting conditions were optimized to obtain the continuous self-assembly of APM monolayers for up to 15 cycles. From an electronic point of view the use of diazonium salts such as APM permit the fabrication of ultrathin transducing layers, being that the immobilized biomolecule is a few nanometers away from the electrode surface. With these characteristics, the authors developed an impedimetric diagnostic device constructed over a silicon-based 4-plotted gold working electrode microchip, with integrated reference electrode and counter electrode. The active biorecognition layer was constructed by electrografting diazotized amino phenyl maleimide, which was subsequently used for the one-step covalent immobilization of IIa-8.0-2x, an epitope peptide specifically selected by our group for presenting the highest aPL-binding activity.

2. Experimental Procedures

2.1. Reagents

Aminophenyl maleimide (APM), sodium nitrite ($NaNO_2$), cysteine (Cys), tetrabutylammonium perchlorate (TBA), N-(3-dimethyl aminopropyl)-N′-ethyl carbodiimide hydrochloride (EDC), N-hydroxysuccinimide (NHS), Dithiothreitol (DTT), 2-morpholinoethanesulfonic acid (MES) buffer, phosphate-buffered saline (PBS), ethylenediaminetetraacetic acid (EDTA) and human serum (H4522) were purchased from Sigma Aldrich. Pierce protein-free T20 blocking buffer (37573) and goat anti-human IgG (H+L) marked with Alexafluor 488 (A11013) were purchased from ThermoFisher. Otherwise stated, all reagents were used without further modification. Standard solutions and buffers were prepared with deionized water (18.2 MΩ.cm at 25°C) obtained from an ELGA water purification system.

2.2. . Peptides and Monoclonal IgG production

The peptide epitope, IIa-8.0-2x (^{1}RSRGGMRKRKKPLTG^{15})$_2$, and the monoclonal IgG have been generated by microwave-assisted PepPower™ peptide synthesis platform and MonoExpress® protocol, respectively, by GenScript Biotech B.V. (Netherlands) (Moghbel et al., 2022).

2.3. Silicon Chip for Electrochemistry

The microchip used in this study features a photolithographed 4x7mm silicon transducer integrated with four gold working electrodes (WE= 0.64 mm^2), two Ag/AgCl reference electrodes (RE=0.13 mm^2), and a central platinum counter electrode (CE= 1.37 mm^2). Silicon technology was fabricated in a clean room at Barcelona Microelectronics Institute (Spain) using a 10 cm in a diameter silicon wafer. The area of the microelectrodes was delimited by an 800 nm thick silicon dioxide prepared by thermal oxidation and the electrodes were photolithographed and lifted off. Subsequently, the metallic areas confined for electrodes were fabricated by physical vapor deposition, photolithography, and lift-off, as follows: Gold-WE features a triple layer surface with 50 nm Ti, 50 nm Ni, and 200 nm Au layers. Platinum-CE was fabricated in a bilayer with 15 nm Ti and 150 nm Pt. Silver-RE was fabricated in a bilayer with 15 nm Ti and 150 nm Ag. The microchip was treated with plasma-enhanced chemical vapor deposition to fabricate a dielectric bilayer consisting of 400 nm SiO_2 and 400 nm of Si_3N_4. Dry reactive ion etching, and photolithography were used to remove the passivation layer from the active microelectrodes area. Finally, the microchip was wire-bonded to a PCB using a Kulicke and Sofa 4523A equipment and insulated using Ep-Tek H70E-2LC epoxy resin.

2.4. Functionalization of the working electrodes

Initially, the microelectrodes were cleaned in a Pico PCCE (Diener, Germany) plasma cleaner at 0.2 mbar (air) for 30 s. After this treatment, APM was electro-grafted onto the gold WEs by promoting the electrochemical reduction of its diazotized cations by cyclic voltammetry (CV). Briefly, the microelectrodes were immersed in a cold acidic solution containing 15mM APM and 3mM $NaNO_2$, and 200 mM TBA, and then, fifteen cycles from +0.4 V to -1.2V were performed with a scanning rate of 0.5 V/s and a step potential of 0.01V. After this step, the immobilization of the IIa-8.0-2x epitope peptide was performed by click chemistry reaction between the thiol of the terminal cysteine of the peptide (activated by dithiothreitol 100 µM) and the electro-grafted maleimide by incubating the microelectrode during 1.5h in a 10 µg/mL PBS/peptide solution. Then, the remaining maleimide groups were inactivated by incubation for 45 min in a 10 mg/mL cysteine solution and passed this time, the unspecific binding sites were blocked by incubation in blocking buffer for 45 min. Finally, the electrodes were washed and stored at 4°C in PBS buffer.

2.5. Sample Preparation

To analyze the matrix effect, the impedimetric response of the electrode was investigated with different concentrations of human serum from 0.05% to 50%. We found that a range from 0.05 to 0.2% serum concentration was optimum to perform the experiments without an extensive matrix blocking effect. Since the expected values of antibodies in a regular sample are in the µg/mL range, we chose to prepare the samples at 0.1% serum concentration corresponding to the 1:1000 dilution of a sample, and therefore, the biosensor performs detections at the picogram/mL range. Two calibration curves were prepared, one analyzed in PBS and the other in HS 1:1000 to calculate the instrumental limit of detection of the biosensor. Sample detection was studied by the standard addition method, for these measurements, a volume of 50 µL of the sample to be quantified was added to each point of the calibration curve prepared in serum at 1:1000.

2.6. Determination of aPL by ELISA

MaxiSorp 96 well plates (Nunc) or Pierce streptavidin-coated high-capacity 96-well plates (Thermofisher) were coated with 10 µg/ml biotinylated-peptide before incubation with aPL samples. Secondary anti-human antibodies conjugated to IR800CW (Rockland) or horseradish peroxidase were used. Protein- or peptide-bound antibodies were detected and quantified by the Odyssey system (Li-Cor Biosciences).

2.7. Electrochemical parameters and characterization.

Electrochemical measurements, cyclic voltammetry (CV), and electrochemical impedance spectroscopy (EIS) techniques were used for characterizations after each functionalization step and for the detection of aPL in human serum samples. The electrochemical measurements were carried out in a 5 mM $K_3[Fe(CN)_6]/K_4[Fe(CN)_6$ solution prepared in PBS (10mM; pH 7.4). CV measurements were performed by scanning the potential from −0.2 to 0.6 V with a scanning rate of 50 mV/s, while the EIS measurements were carried out in a range of frequency from 100 mHz to 100kHz with a DC potential of 10 mV and an AC potential of 10 mV. Measurements were effectuated inside a faraday cage using a PalmSens 4 (Netherlands) adapted with a multiplexor device. The spectra were recorded in PSTrace 5.7 software. EIS spectra obtained as a Nyquist plot in the form of deformed semicircles were analysed with Zviewer software to perform a mathematically fitting of the results according to the electrical circuit Rs (Q Rc W). Where Rs is the resistance of the solution, Q is the phase constant element (a pseudo capacitance of the double capacitive layer), Rct is the charge transfer resistance related to the interface of the biosensor and the redox probe and W is the Warburg impedance in relation of the diffusive processes of the redox probe at the surface.

2.8. Fluorescent Characterization

After electrochemical detection, the microelectrodes were stained overnight at 4°C with 4µg/mL of goat anti-human IgG (H+L) conjugated with Alexafluor 488 (A11013; ThermoScientific). The electrodes were then rinsed with PBS and dried before their microscopic analysis with an EVOS M5000 (Invitrogen/ThermoScientific).

3. RESULTS

3.1. Biosensor Construction.

The process of electrografting was investigated in real-time by cyclic voltammetry and the recorded spectra are shown in Fig. 1. In previous publications, other authors have found that after the initial reduction cycle, the multilayer growth occurs only as non-catalyzed process, therefore the thickness of the deposed film cannot be fully controlled (Harper et al., 2008). In our results from the very first cycle, we observe irreversible reduction peaks at -0.84, related to the electrocatalytic reaction, and at -1 V related to the non-catalyzed reaction after the grafting of the monolayer is established. This phenomenon could also be explained by the presence of different sites with different reactivities as the surface is being modified becoming more insulating. After each cycle the variations in current start to diminish gradually following Cottrell's equation up to electrode passivation. This behavior indicates that the grafting of the layers occurs in a catalyzed manner until the precursor can no longer interact directly with the gold electrode, suggesting that the reaction performed in acidic solution begins with the

formation of nitrous acid by the reaction of NO_2^- and H^+. After stabilization, the highly reactive nitrosonium ion is prone to the nucleophilic attack of the primary amine present in APM creating the diazonium ion, which is then, strategically reduced by cyclic voltammetry to be attached to the gold surface.

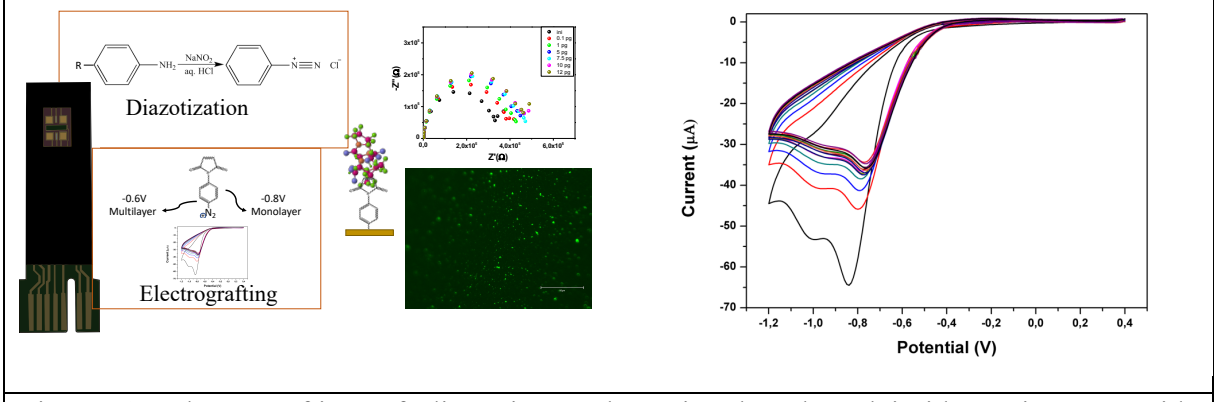

Figure 1. Electrografting of diazonium salt aminophenyl maleimide, epitope peptide immobilization and detection of aPL.

During the fabrication process of the biosensor, the surface of the electrode was studied through CV and EIS. In Fig. 2A in the black line, we observe the initial voltammogram of the clean electrode characterized by the reversible reaction of the redox probe. In the blue line, after the electrografting of APM we notice a drastic reduction in conductivity. After click immobilization of the epitope aptamer, we noticed a small decrease in conductivity and after the blocking process, we noticed that the most insulating characteristic of the sensor surface is attained with another reduction of conductivity. Similarly, the analysis by EIS (Fig. 2B) demonstrated increases in the overall impedance of the sensing surface represented in the Nyquist plot by the increasing height of the semicircles. The impedimetric responses offer more information about the processes occurring at the interface of the electrode in relation to the behavior of the redox probe. Mathematically the semicircles were analyzed by fitting them to the electrical behavior of the equivalent circuit RQRW.

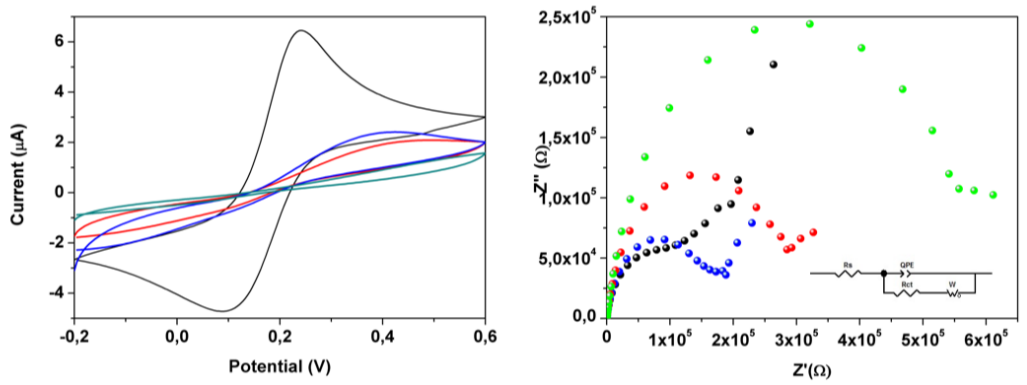

Figure 2. CV characterization in Ferrocyanide black) clean; blue) APM deposition; red) peptide immobilization; green) blocked electrode.

3.2. Analytical Performance of the Biosensor.

The biosensors were tested with human serum samples through the standard addition method and the responses were studied by their mathematical fitting to the RQRW equivalent circuit. To compare the responses within different electrodes, R_{CT} values were normalized as, $\%\Delta R_{CT} = \left|\frac{RCT_{((\text{serum anti IIa}-8.0-2x)} - RCT_{(\text{IIa}-8.0-2x)}}{RCT_{(\text{IIa}-8.0-2x)}}\right| \times 100$. In Fig. 3 red circles, we present the calibration curve performed in PBS, ΔR_{CT} values increase gradually to the concentration of anti-IIa-8.0-2x according to the equation $\%\Delta R_{CT}$= 4.92 + 2.73 (Anti IIa-8.0-2x pg/mL), r^2=0.94. In green circles, we present the calibration curve performed in serum 1/1000. Similarly, ΔR_{CT} values increase gradually to the concentration of anti-IIa-8.0-2x according to the equation $\%\Delta R_{CT}$= 73.66 + 36.19 (Anti-IIa-8.0-2x pg/mL), r^2=0.99. In this curve, we observe the effect that the presence of the matrix has on the %RCT, from this curve we calculated the limit of detection as LOD= 3.33 σ/S, where σ is the S.D. of the value of the intercept (σ=8.86) and S is the slope of the curve, therefore LOD was calculated as 0.8 pg/mL. In blue circles we present the result of the standard addition method prepared with a 7.5 pg/mL anti-IIa-8.0-2x sample. The results were fitted according to the equation $\%\Delta R_{CT}$= 347.80 + 45.02 (Anti IIa-8.0-2x pg/mL), r^2=0.99. From this analysis, we obtained a calculated concentration of 7.7±0.14 pg/mL. These promising results show that the immobilization technique performed by the electro grafting of the amino phenyl maleimide is crucial to maintain the biological activity of the epitope peptide, which requires to be spatially oriented upwards to be able to perform the recognition of aPL.

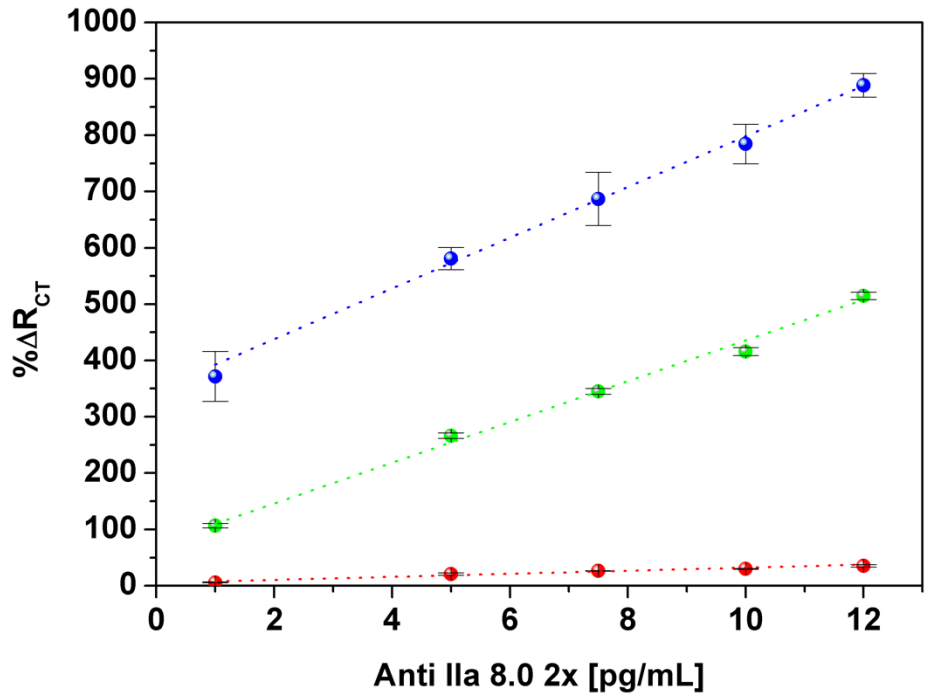

Figure 3. Calibration curves prepared in, red circles) pure PBS; green circles) HS 1/1000; blue) standard additional method with a 7.5 pg/mL concentration of anti-IIa 8.0 2x antibody in HS 1/1000.

After testing the biosensor by the standard addition method, the microelectrode was incubated in a solution of fluorescently marked anti-human antibody to reveal the actual captured anti-IIa-8.0-2x antibody over the surface of the working electrodes. In Fig. 4 we show the analysis of the 4 working electrodes. The fluorescent labeling was observed mainly as small green, fluorescent spots; however, some big fluorescent agglomerations could be observed as well. From this result, we conclude that the anti-IIa-8.0-2x antibody was captured from the samples prepared in 1/1000 HS.

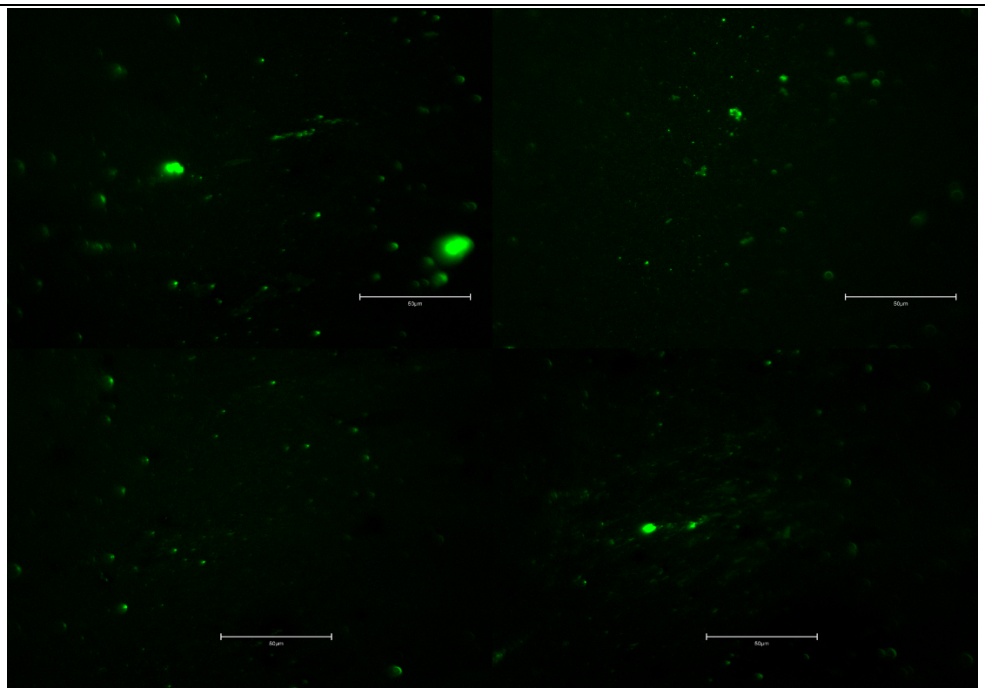

Figure 4. Fluorescence microscopy of 4 micro working electrodes labeled with fluorescently labeled anti-human secondary antibody.

3.3. Practical application of the biosensor for aPL detection in patient samples.

After the positive confirmation of the feasibility of our biosensor, we proceeded to analyze a real serum sample from patient by the standard addition method in double blinded study. In Fig. 5 we show the calibration curve, fluorescence microscopy and expected concentration of the tested serum sample. From the Nyquist plots shown in Fig. 5a we performed the mathematical fitting to obtain the R_{CT} values. Subsequently, the normalization of the results to $\Delta R_{CT}\%$ were plotted vs. concentration to obtain the equation $\Delta R_{CT}\% = 19.27+1.79$ (aPL pg/mL), $R^2=0.91$. The concentration value of the tested sample was calculated by solving the equation when $\Delta R_{CT}\%=0$, as a result, we obtained 10.7 ng/mL (after applying the dilution factor). The expected ELISA concentration was 9.5 ng/mL, therefore a recovery of 112 % was obtained.

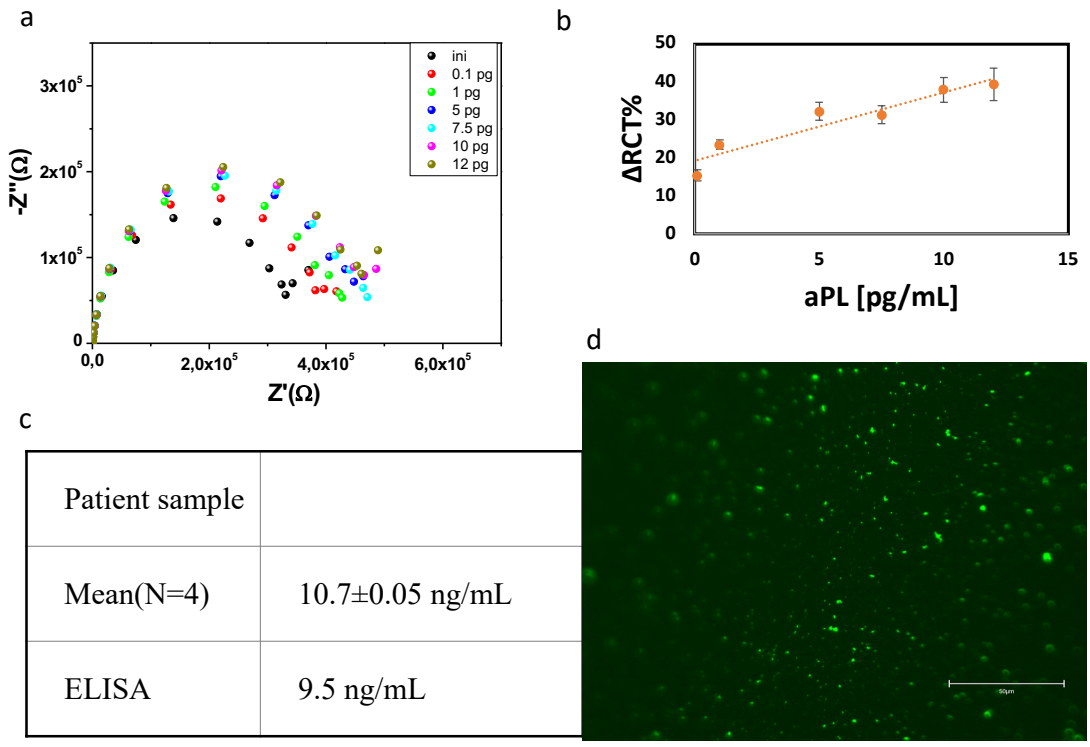

Patient sample	
Mean(N=4)	10.7±0.05 ng/mL
ELISA	9.5 ng/mL

Figure 5. Calibration curve of a patient's sample measured with the biosensor by the standard addition method.

4. CONCLUSION

A micro-integrated biosensor for the detection of anti-IIa-8.0-2x antibody was constructed based on click chemistry modification of the working electrode surfaces. Initially, the click-to-thiol molecule aminophenyl maleimide was efficiently grafted by electrocatalysis, a common drawback reported as a limiting factor for the use of diazonium salts in gold surfaces. Thiol-activated peptide aptamer was then immobilized over the surface for the specific detection of the antibodies. The biosensor was tested in human serum samples and showed good performance to quantify anti-IIa-8.0-2x antibody at the pg/mL range. After studying patient's serum sample and applying the dilution factor, the biosensor reported values close to the ELISA result.

5. REFERENCES

Alijotas-Reig, J., Esteve-Valverde, E., Anunciación-Llunell, A., Marques-Soares, J., Pardos-Gea, J., Miró-Mur, F., 2022. Pathogenesis, diagnosis and management of obstetric antiphospholipid syndrome: A comprehensive review. J Clin Med 11, 675.

Gerardi, M.C., Fernandes, M.A., Tincani, A., Andreoli, L., 2018. Obstetric anti-phospholipid syndrome: state of the art. Curr Rheumatol Rep 20, 1–12.
Harper, J.C., Polsky, R., Wheeler, D.R., Brozik, S.M., 2008. Maleimide-Activated Aryl Diazonium Salts for Electrode Surface Functionalization with Biological and Redox-Active Molecules. Langmuir 24, 2206–2211. https://doi.org/10.1021/la702613e
Hetemi, D., Noël, V., Pinson, J., 2020. Grafting of Diazonium Salts on Surfaces: Application to Biosensors. Biosensors (Basel) 10, 4. https://doi.org/10.3390/bios10010004
Miyakis, S., Lockshin, M.D., Atsumi, T., Branch, D.W., Brey, R.L., Cervera, R., Derksen, R.H.W.M., de Groot, P.G., Koike, T., Meroni, P.L., 2006. International consensus statement on an update of the classification criteria for definite antiphospholipid syndrome (APS). Journal of thrombosis and haemostasis 4, 295–306.
Moghbel, M., Roth, A., Baptista, D., Miteva, K., Burger, F., Montecucco, F., Vuilleumier, N., Mach, F., Brandt, K.J., 2022. Epitope of antiphospholipid antibodies retrieved from peptide microarray based on R39-R43 of β2-glycoprotein I. Res Pract Thromb Haemost 6, e12828. https://doi.org/https://doi.org/10.1002/rth2.12828
Saccone, G., Berghella, V., Maruotti, G.M., Ghi, T., Rizzo, G., Simonazzi, G., Rizzo, N., Facchinetti, F., Dall'Asta, A., Visentin, S., 2017. Antiphospholipid antibody profile based obstetric outcomes of primary antiphospholipid syndrome: the PREGNANTS study. Am J Obstet Gynecol 216, 525-e1.

CHAPTER V

GENERAL DISCUSSION, CONCLUSION AND PERSPECTIVES

In this thesis we have approached, to the best of our knowledge and technical capacities, the development of flexible biosensors. We worked in partnership with high-end industries in the top of the development of carbon-based flexible biosensors and biomedical diagnostics. We developed material science, chemical and engineering solutions for the most common drawbacks that are being faced by scientist willing to develop economic, sensitive, and specific flexible biosensors. Society, as the end user of flexible biosensors, requires straightforward and ready to use diagnostics. Foreseeing the large use of these promising devices, their development is staged gradually from selection of the biomarker and the study of its biorecognition abilities in the solid state. Following with the selection of the main sample to be used in the diagnosis, the transducer and substrate of the biosensor must be designed accordingly. If these kinds of biosensors are to reach the primary level of health services or pharmacy bench, the materials used in their construction must be almost innocuous to the environment, reflecting recyclability or better yet, biodegradability. Sometimes, the complexity in the post-treatment of the devices represent obstacles as big as the requirements of high sensibility and easy manipulation. We have found in the literature, that the transducing materials start to being studied in solid state, then flexible to continue to stretchable materials. In this thesis we explored the use of graphene foam, which is an intrinsic conductive material that presents flexible and stretchable mechanical characteristics aligned with flexible and stretchable substrates. Regularly, using pure graphene as a transducer is overlooked because of its hydrophobicity and the stacking of the graphene layers. In this context, the non-covalent π-π functionalization that is presented here allows to maintain the electronic properties of graphene. With this strategy, the impedimetric measurements were conducted in simple PBS buffer attaining a limit of detection (LOD) of 7.89 fg/mL in artificial saliva. After measurement, PBS can be sterilized and simply discarded in the drainage. This kind of research impact directly, the overall economic and environmental cost that the global use of biosensors might have at a large scale.

Continuing with the development of π-π adsorption, we selected commercial screen-printed carbon electrodes because of their availability. These kinds of sensors are known for their modest performance; however, we developed a conditioning method by electrochemically reducing the oxidated chemical species of the sp^2 in carbon ink. Although, conductivity was increase, we discovered that this simple treatment is not enough to match the electronic properties of graphene, for that reason we required the use of oligonucleotide aptamers as exceptional biomolecular probes. These specific oligonucleotide aptamers are an outstanding biological strategy to mediate fast electron transfer by migration of charge from the double-

layer capacitance to the carbon transducer. It is with these two strategies that commercial SCPE were enhanced to detect antibodies in blood serum in concentrations as low as 0.8 pg/mL.

Regarding the argument over which kind of biosensors are apt to reach commercial value, we should consider that the use interleukins profiles as excellent prognosis and diagnosis biomarkers, their quantification via antibodies can be rapidly transferred to almost any know biosensing platform. However, not every biological probe can perform biorecognition in anisotropic conditions. For instance, we presented a peptide aptamer requiring specific position immobilization to perform its biorecognition function. For this research, we aimed to overcome several challenges at a time. For instance, sputtered gold films are still considered promising transducers to be used in flexible biosensors, at the same time, the electrodeposition of diazonium salts onto gold is still considered to be weak and unreproducible. Because of the big challenge, we decided to start the exploratory research in a silicon microchip whose working electrodes are gold films deposited by plasma chemical deposition, to initially avoid the interference of the flexible substrate. As a result, we obtained a reproducible methodology to produce layer-by-layer electrodeposition of maleimide diazonium salts. With this approach the peptide aptamer was tethered in high orientation to enhance its biological functionality.

As perspectives of this work, we understand that flexible biosensors are developed to perform *in situ* analysis and their requirements are becoming more personalized, and patient controlled. Therefore, these devices are advancing in the direction of self-powered wearable biosensors, dismissing the need of external electronic power or rechargeable batteries. Fortunately, flexible graphene electrodes can also serve as the anode for flexible lithium batteries. The energy required to power these devices can be harvested from heat, vibration, light, radio frequency, chemicals, or capillary pumping. Biofuel cells have been used to power wearable biosensors, most of them rely in the enzymatic reaction they are design to detect (glucose or lactate). However, the potentials generated are not sufficiently high or constant (0.44 and 0.46 V, respectively). As an alternative strategy, including graphene micro supercapacitors (MSC) integrated in the sensing systems that can be repeatedly charged by integrated wireless radio frequency power receivers are some of the aspects that could be explored in future works.